AD_____

AWARD NUMBER: W81XWH-04-1-0589

TITLE: Elastic Scattering Spectroscopy for the Detection of Pre-Cancer and Early Cancer of the Breast

PRINCIPAL INVESTIGATOR: Stephen G. Brown

CONTRACTING ORGANIZATION: University College London
London WC1E 6BT United Kingdom

REPORT DATE: June 2006

TYPE OF REPORT: Final

PREPARED FOR: U.S. Army Medical Research and Materiel Command
Fort Detrick, Maryland 21702-5012

REPORT DOCUMENTATION PAGE

Form Approved
OMB No. 0704-0188

1. REPORT DATE *(DD-MM-YYYY)*	**2. REPORT TYPE**	**3. DATES COVERED** *(From - To)*
01-06-2006	Final	1 Jun 2004 – 31 May 2006

4. TITLE AND SUBTITLE

Elastic Scattering Spectroscopy for the Detection of Pre-Cancer and Early Cancer of the Breast

5a. CONTRACT NUMBER

5b. GRANT NUMBER
W81XWH-04-1-0589

5c. PROGRAM ELEMENT NUMBER

6. AUTHOR(S)

Stephen G. Brown

E-Mail: s.bown@ucl.ac.uk

5d. PROJECT NUMBER

5e. TASK NUMBER

5f. WORK UNIT NUMBER

7. PERFORMING ORGANIZATION NAME(S) AND ADDRESS(ES)

University College London
London WC1E 6BT United Kingdom

8. PERFORMING ORGANIZATION REPORT NUMBER

9. SPONSORING / MONITORING AGENCY NAME(S) AND ADDRESS(ES)
U.S. Army Medical Research and Materiel Command
Fort Detrick, Maryland 21702-5012

10. SPONSOR/MONITOR'S ACRONYM(S)

11. SPONSOR/MONITOR'S REPORT NUMBER(S)

12. DISTRIBUTION / AVAILABILITY STATEMENT
Approved for Public Release; Distribution Unlimited

13. SUPPLEMENTARY NOTES

14. ABSTRACT

Elastic scattering spectroscopy (ESS) interrogates tissue with short pulses of white light, obtaining diagnostic information from immediate spectral analysis of light scattered back. From data pairs correlating spectra with conventional histology at individual points, we developed diagnostic algorithms to detect cancer by spectral analysis. Pixels containing less than 20% cancer were detected in mastectomy specimens. In initial testing on axillary nodes, some cancers were missed due to inadequate sampling. This was addressed by scanning the cut surface of excised sentinel nodes (400 pixels/cm2) to create an optical image which improved sensitivity to 77.8% with 97.5% specificity. This is comparable to touch imprint cytology, an established technique for rapid assessment of nodes, but with no need for tissue processing or for a pathologist's opinion. Greater sensitivity should be possible by scanning more layers of nodes (ESS interrogates 0.3-0.5mm into tissue). Preliminary studies suggest that ESS may also be able to diagnose lesions seen at ductoscopy (where biopsy is not feasible) and detect aneuploidy, an important prognostic factor. These results justify further prospective studies. The technique is simple in concept, uses low cost equipment and has considerable potential for the immediate detection of cancer in vivo or ex vivo in many tissues.

15. SUBJECT TERMS
Elastic scattering spectroscopy, optical biopsy, breast cancer, sentinel node, ductoscopy, ploidy, scanning

16. SECURITY CLASSIFICATION OF:			**17. LIMITATION OF ABSTRACT**	**18. NUMBER OF PAGES**	**19a. NAME OF RESPONSIBLE PERSON**
a. REPORT	**b. ABSTRACT**	**c. THIS PAGE**			**19b. TELEPHONE NUMBER** *(include area code)*
U	U	U	UU	63	USAMRMC

Standard Form 298 (Rev. 8-98)
Prescribed by ANSI Std. Z39.18

Table of Contents

INTRODUCTION

Breast cancer remains the most common malignancy affecting women within the western world, and until recently accounted for the highest number of cancer deaths in women. Epidemiological data shows an ongoing rise in the incidence within the western world, though within recent years there have been modest improvements in mortality.

Widespread mammographic screening and greater public awareness of breast cancer as a result of effective education campaigns are resulting in earlier presentation of breast cancer. Early diagnosis of breast cancer prior to the development of metastases enables more conservative treatment and results in a greater chance of cure.

The focus of this research program is the development of an optical technique called elastic scattering spectroscopy (ESS) for detection, assessing the extent of spread (staging) and prognostication of early breast cancer.

Numerous optical methods of diagnosis are under investigation worldwide(1). The key advantages of optical techniques such as ESS are:
- Speed of diagnosis: Since computer based algorithms can be developed for spectral analysis, a near instantaneous result is achievable
- No highly trained operator is required for measurements or analysis
- Safety: Avoids the use of ionizing radiation for diagnosis
- No tissue loss: Analysis by optical measures is non-destructive to tissue; hence tissue can be re-analyzed conventionally to confirm accuracy

Elastic scattering spectroscopy has further advantages, which include:
- ESS indirectly measures cellular and subcellular changes within tissue, hence making it ideal for detection of malignant change
- Low cost equipment
- Portability: The system can be easily transported and set up within the clinic or operating room
- Diagnostic information obtained from deeper layers: The system uses information gathered down to approximately 0.3mm in depth from the tissue surface.

Theoretical Background to Elastic Scattering Spectroscopy

The principle of elastic scattering spectroscopy (ESS) is that tissue is interrogated by short pulses of white light, delivered by a thin optical fiber just touching the tissue surface. The light scattered by the tissue is collected by a second fiber immediately adjacent to the first (center-centre 0.35mm) and the diagnostic information obtained by statistical analysis of the spectrum of the scattered light.

When performed using an appropriate optical geometry, the spectrum is sensitive to the sizes, indices of refraction and structures of the sub-cellular components (eg nucleus, nucleolus and

mitochondria) that change with malignant transformation(2;3). The measured ESS spectra relates to the wavelength-dependence and angular-probability of the scattering efficiency of tissue micro-components (as well as to absorption bands) based on the fact that many tissue pathologies and most cancers undergo such morphological changes at the cellular and sub-cellular level.

Consequently this approach generates spectral signatures, which reflect the tissue parameters that pathologists address, such as the size and shape of nuclei and organelles, the nucleo-cytoplasmic ratio and chromatin density. Statistical analysis can be used to recognize patterns within the spectra, which can then be used to discriminate between spectra from malignant and benign tissue once appropriate diagnostic algorithms have been developed. Both Mie theory and finite-difference time domain methods have been employed successfully to model spectral changes resulting from malignant transformation.

Elastic Scattering Spectroscopy Equipment

The ESS instrumentation consists of a pulsed xenon arc lamp, a spectrometer, an optical probe and a computer to control the various components and record the spectra. The arc lamp, spectrometer and power supply are housed in a briefcase size unit to which the laptop computer is connected. ESS involves directing short pulses of white light (320-920nm) from a pulsed xenon arc lamp (Perkin Elmer, Inc.) through a flexible optical fiber touching the tissue to be interrogated. Ultraviolet B (280-315nm) and ultraviolet C (100-280nm) light is filtered out to avoid any potential risk to patients if used in-vivo.

A collection fiber, with a fixed separation distance of ~350 μm from the first, collects light scattered from the upper layers of the tissue and propagates it to the spectrometer (S2000 Ocean Optics) which outputs the spectrum to the laptop computer for recording and further analysis.

Figure 1 shows a schematic diagram of the system; figure 2 shows a photograph of the system and figure 3 shows a depiction of the optical geometry employed within the system. Typically, the whole fiber assembly measures 1.5 mm and the distal end may be housed in a rigid stainless steel casing for easy handling and sterilization. The collection and recording of a single spectrum takes less than a quarter of a second

.

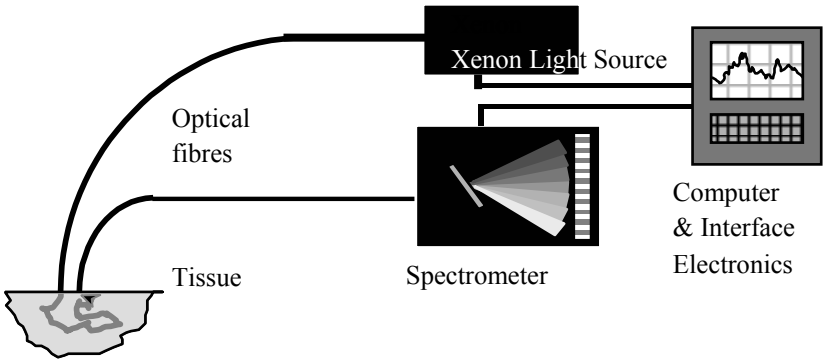

Figure 1. Schematic diagram of Elastic Scattering Spectroscopy (ESS) system.

Figure 2. Photograph of ESS Optical Biopsy System

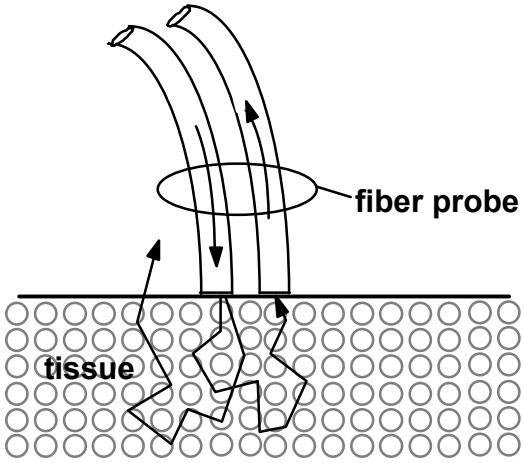

Figure 3. Depiction of the optical geometry used in the ESS method. Fiber tips are in optical contact with the tissue surface. With a fiber separation of ≤350 microns (center-to-center) only light that has scattered elastically a small number of times, and at large angle within a shallow layer is collected.

Before any spectra are taken, a white reference spectrum is recorded. The reference spectrum establishes the system response by recording the diffuse reflectance from a flat surface of Spectralon^{TM} (Labsphere Inc.). Spectralon has a spectrally flat reflectance between 250 and 1000 nm. The reference spectrum allows variation in the light source, spectrometer, fiber transmission and fiber coupling to be accounted for. Each recorded ESS spectrum from tissue is divided by this reference spectrum to give a system-independent measurement for the site being investigated.

BODY

REGULATORY ASPECTS

The program received ethics committee (Institutional Review Board) approval from the Joint University College London and University College London Hospitals Ethics committee.

The program was submitted as 2 separate ethics applications:

1. Optical biopsy utilizing elastic scattering spectroscopy for early diagnosis, staging and prognostication in breast cancer (Short title : Optical Biopsy for Diagnosis, Staging & Prognosis in Breast Cancer). A favorable ethical opinion was given on the 17th of November 2004, under reference number 04/Q0502/83. Trust research and development approval for this study was granted on the 21st January 2005 under reference number 04/0109.
2. Ex-vivo ductoscopy with elastic scattering spectroscopy for the diagnosis of ductoscopic abnormalities and light dosimetry studies (Short title: Light for diagnosis and treatment of ductoscopic abnormalities). A favorable ethical opinion was given on the 19th of November 2004, under reference number 04/Q0502/40. Trust research and development approval for this study was granted on the 21st January 2005 under reference number 04/0209. A separate sub-protocol of light dosimetry experiments unrelated to this particular program was included within this ethics application.

A further ethics application will need to be submitted in the future for the in-vivo ductoscopy work, though we do not currently have sufficient data from the ex-vivo study to support this application, so this was not feasible during the period of this grant.

An independent Human Subjects Protection Review was conducted by the USAMRMC Office of Research Protections, on the 13th of July 2005, under reference numbers A-12727-1 and A-12727-2. The protocols were finally approved following minor revisions to these.

Prior to the final approval by the USAMRMC Office of Research Protections, money from this grant could not be used to support Dr Chicken's clinical work, but alternative resources were available to cover this period. Since final approval was granted, Dr Chicken's clinical work has been supported from the grant.

The delays in obtaining ethical approval were due mainly to the complete restructuring of the system throughout the European Union, to make the procedures uniform in all 25 countries. The new procedures are far more complex than the old ones. Much of the delay was because those administering the new system did not have the necessary guidelines on how to proceed. Once these were made available, there were further delays due to the backlog of applications that had built up. Our application could not be considered by the USAMRMC Office of Research Protections until it had been approved locally in the UK.

PERSONNEL

Dr Kristie Johnson (physicist) resigned to take up a position in Sydney, Australia, and was replaced by Dr Benjamin Clark (physicist). Dr Clark resigned in October 2005 to take up a position at Imperial College in London, and was replaced by Dr Martin Austwick (physicist). Dr Austwick's Curriculum Vitae is attached to the report as an appendix. Apart from this, all personnel remain as identified in the original proposal.

AIMS AND RATIONALE OF RESEARCH

This research program had 4 primary aims:

1. To refine algorithms and develop new techniques for analysis of ESS (elastic scattering spectroscopy) spectra

2. To develop elastic scattering spectroscopy for the immediate detection of metastatic cancer in axillary sentinel lymph nodes. The sentinel node is any node with direct lymphatic drainage from a primary tumour and is by definition the first node to be involved when lymphatic metastases occur. Sentinel node biopsy is an accurate procedure for lymphatic staging in breast cancer that avoids the morbidity of full axillary lymph node dissection in node negative patients. The rationale for this part of the study is that patients with sentinel node metastases require axillary lymph node dissection (clearance) for regional control of the disease. Unless sentinel node metastases can be diagnosed at the time of sentinel node biopsy, a second operation is required for axillary lymph node dissection, with its associated psychological and economic costs and consequent delay in commencement of adjuvant therapies. Existing means for intraoperative detection of sentinel node metastases (frozen section, touch imprint cytology) rely on the expert opinion of a pathologist and typically take at least 30 minutes for a result.

3. To develop elastic scattering spectroscopy for the detection of aneuploidy. The rationale for this is that ploidy shows promise as an independent prognostic marker in breast cancer. Laboratory determination of ploidy is however time consuming and requires expensive equipment. ESS may offer a rapid and simple alternative.

4. To develop elastic scattering spectroscopy for diagnosis of pathology visualized at ductoscopy. Ductoscopes are small caliber fibre-optic endoscopes which are introduced into the ductal system through the nipple. 80% of breast cancers are ductal in origin. Ductoscopy may be used to detect very small tumors (as small as 0.2mm) or pre-invasive changes such as ductal carcinoma in situ (DCIS). A role for ductoscopy has been suggested in determining appropriate margins for excision of tumors as well as for the assessment of blood stained nipple discharge, which may be a presenting symptom of breast cancer. The rationale for this part of the study is that the small caliber of ductoscopes prevents taking histological samples for confirmation of the diagnosis. Optical biopsy may offer the ability for instant diagnosis, and in the longer term, potentially, immediate therapy.

Objective 1. New techniques for analyzing data pairs from our existing database on breast tissue.

a) Review biopsies from the existing database to quantify the extent of each type of normal and neoplastic tissue in each.
b) Develop new diagnostic algorithms for spectra from sites where the biopsies contain predominantly only one type of tissue to discriminate between normal and malignant tissue.
c) Use the new algorithms to test spectra from sites where the biopsies contain both normal and malignant tissue to assess whether small areas of cancer can be detected.

Current Method for Analysis of Spectra

Previous analytical methods used model based feature extraction. We have now developed a purely statistical approach to spectral analysis using discriminant analysis.

Currently, the analysis consists of:

1. Cropping spectra from 400-800nm to remove uninformative regions (regions at the end of the spectrum where the signal:noise ratio is low).
2. Combing the spectra to reduce the number of measurements.
3. Smoothing by the Savisky-Golay method
4. Removal of spectra negatively saturated at the hemoglobin peaks
5. Normalisation/Standardisation of spectra using the standard normal variate method. This consists of subtracting the mean intensity and dividing by the standard deviation of the spectrum, giving spectra with a mean of zero and a variance of ±1.
6. Data compression using Principal Component Analysis (PCA)
7. Discriminant analysis using Linear Discriminant Analysis (LDA). The number of principle components used is determined by either a forward stepwise method, or a pragmatic search of the possible combinations of principle components.
8. The data is then split into a training set and test set and the final LDA analysis is run on the data and the test set results are recorded.
9. Models are validated using re-sampling techniques whereby different training/test set combinations are randomly assembled and the analysis is repeated, yielding an estimate of the behavior of the algorithm on average.
10. For each model, the trade-off between sensitivity and specificity is visualized using a receiver-operator curve (ROC curve). This is calculated by altering the canonical scores (from an LDA or QDA). Once the relationship between sensitivity and specificity has been estimated, an appropriate cutoff point can be decided upon. The final algorithm consists of PCA loadings, and Discriminant analysis coefficients (Canonical Coefficients, or Classification Coefficients) and the cutoff canonical score.

Algorithms are run in Systat (SYSTA Software Inc), Matlab (Mathworks), or GNU R (R development core team).

We have investigated several alternative analytical methods :

1. Partial least squared squares regression analysis is a multivariate technique which can be used to relate several response (Y) variables to several explanatory (X) variables. The method aims to identify the underlying factors, or linear combination of the X variables, which best model the Y dependent variables. In practice, this technique is complicated and has high computational requirements, and is therefore slow to produce results.

2. Soft independent modeling of class analogy (SIMCA) is a statistical method based on construction of mathematical descriptions of clusters of data. It uses PCA as a starting point. New data is identified by its position within a cluster. We have applied this methodology in the analysis of our ESS scanner data to extract the measurements taken from the nodes from those taken from the background.

3. A novel method modeling measurement variability, and extracting this variability from the spectra prior to attempting discrimination has been developed. This has been successfully applied to collateral work on using ESS in Barretts esophagus, resulting in enhanced detection of dysplasia. A demonstration of this approach applied to breast cancer is shown below within the proof of principle study. We plan to use this method in the future on ESS scans with multiple measurements at each site.

Proof of Principle Study

In an early study in the program we undertook a detailed analysis of large sections taken through cancers removed by mastectomy. ESS measurements were taken on an 8 by 8 grid (each pixel 2x2mm). Subsequently our histopathologist gave a detailed report, which included documenting the amount of cancer present in each pixel. By correlating the spectral measurements and the histological diagnosis, we aimed to estimate the sensitivity of the ESS device in detecting cancer. During the earlier study, the raw data from histology and ESS were obtained, but the spectral analysis was not completed. That has been done as part of the present study. In particular, we have tried to determine the smallest amount of tumor present in individual pixels that could be detected. The current analysis is based on data from five ductal cancers, yielding a total of 271 data pairs (spectral measurements and histology).

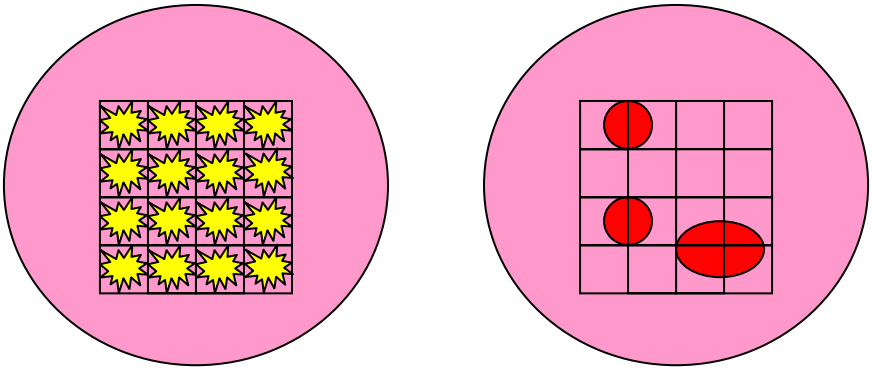

Figure 4 Schematic diagram of the grid experiment. Left: Spectral measurements were taken on a grid. Right: form of mapping of cancer areas

The grid data were analyzed with the aim of determining whether the model was capable of detecting cancer at sites where a large proportion of the tissue interrogated by the light pulses was normal. In this analysis, the model was trained on a subset of the spectra from either 100% normal (0% cancer) tissue, or 80-100% cancer. The remaining spectra were then used as a test set to assess the performance of the algorithm.

Four of the 30 principal components used in this analysis are shown plotted against each other in figure 5. A particular feature of this dataset not seen in the sentinel node study can be seen in the way that data from different sites (shown in different colors) separated out (clustered). In this context, a site is the region of breast tissue from one patient covered by the grid that contains both normal and tumor tissue. The reason that we can see this separation is due to the relatively large numbers of measurements (~ 52 per site) being taken from relatively few sites (5). In addition, the variable amount of cancer in each pixel across sites means that discrimination between normal tissue and cancer may be difficult to distinguish from discrimination between the different tumor containing sites. From the data collected so far, it is difficult to say what physical differences contribute to this "site" effect, but it is clear that we should avoid using spectral features that may be confounded by other factors. Preliminary analysis of the parts of the spectrum that contribute to this "site" effect indicate that differences in the amount of absorbance in the region of the Q-band of hemoglobin ~530 nm - ~620nm are mainly explained by site, and consequently differences in blood saturation and oxygenation may vary widely between tumors. There is a clear need to understand the mechanistic basis of the optical differences between normal and malignant breast tissue. We are planning phantom studies to identify the spectral signatures of major components of the tissue.

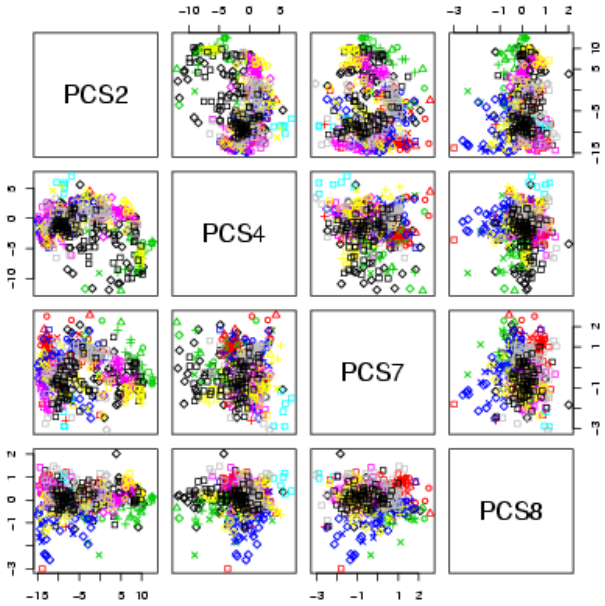

Figure 5. A pairs plot of four principal components that discriminate between sites. Each individual plot contains all of the spectra from each site (from tumor and normal areas) plotted using two principal components. On each of the plots, each site is shown in a different color. Because some of the spectral information is correlated with site of origin, spectra from a single site (i.e. from the same tumor and the immediately surrounding tissue) cluster together, leading to patches of symbols of the same color.

A naive first analysis shows that the probability of detecting tissue with small amounts of cancer in it (1-20%) is roughly 50%. Tissue with large amounts of cancer in it is classified correctly roughly 90% of the time (fig 6a). We attempted to remove parts of the spectrum in which the variance is mainly explained by site, leaving regions where the information is less confounded by the tumor of origin (i.e. with less confusing information in them). We did this by fitting a linear mixed-effects model to the data set at each point in the spectrum. At each point we calculated the amount of variance in the data explained by site, and the amount of variance left over (the *residual variance*) once this *random effect* had been estimated. By looking at the ratio of residual: site variance, we have a measure of how much the variance (at any given point in the spectrum) is explained by site. We removed the regions where the residual: site ratio was below 1 (because this meant that most of the variance was explained by site) and re-ran the analysis with this transformed data. The overall sensitivity and specificity of the model improved slightly (fig 6b, Table 1). The regions of the spectrum removed are indicated in fig 7.

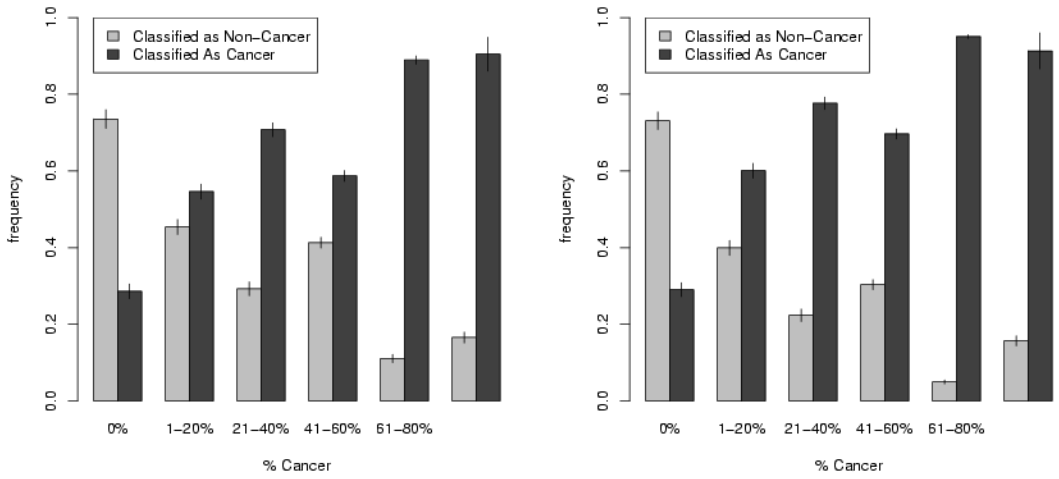

Figure 6 a) Result of the Linear Discriminant Analysis in a model with all parts of the spectra left in. b) Result of the Linear Discriminant Analysis in a model with some parts of the spectrum (shown in Figure) taken out in order to aid discrimination between tumor and normal. In comparison to the complete model (shown in 5a), the discrimination is slightly improved.

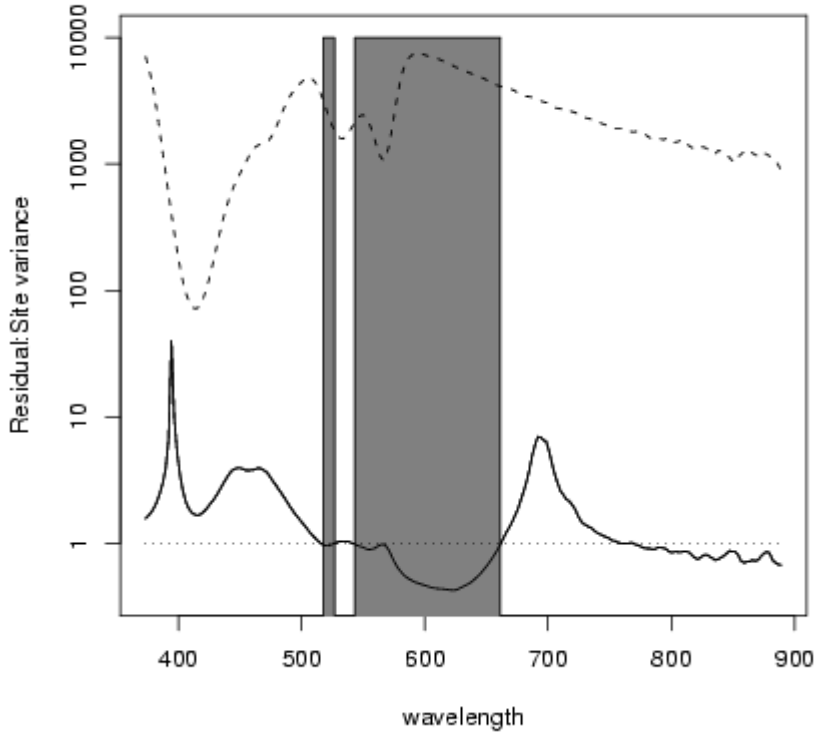

Figure 7 Line plot showing which regions contain useful information, and which regions contain information that is confounded by site. The solid line is the ratio of the residual variance: variance explained by site. The grey regions denote those parts of the spectra where most variance is explained by site of origin rather than anything else. The horizontal dotted line is where the ratio between residual variance and variance explained by site is equal to one. The region > 780 nm was left in as it improved the analysis. The dashed line is a typical spectrum (offset for clarity).

Table 1: The percentage of samples classified as cancer is an increasing function of the amount of cancer in that tissue. The small number of samples with 80-100% cancer may be reflected in the relatively low accuracy in that category (compared to those samples with 61-80% cancer, for example). When the regions shown in Figure are removed, the overall accuracy of the model improves.

	% Cancer in tissue	0%	1-20%	21-40%	41-60%	61-80%	81-100%
% Classified as Cancer	With regions left in	29	51	69	59	90	86
	With regions taken out	29	56	74	67	95	87

The results presented above have potential implications beyond the grid dataset. If some parts of the spectrum are uninformative, or are confounded with other factors such as the site of origin, identifying these regions and controlling for them or removing them would improve our ability to discriminate between normal tissue and cancer. In order to identify these regions we need enough measurements per site in order to distinguish between the effect of differences between sites and the effect of differences within a site. For the sentinel node work (before we started using the scanner), we collected 16 spectra per node as part of the routine measurements, so will be able to use this data to attempt to quantify these regions, although any way of increasing the number of spectra taken from each node will benefit this analysis.

One possible area for future investigation is to identify the physical factors that contribute to this "site" effect and remove them by modeling the absorption of that factor and deducting it from the spectra, leaving the remainder of the spectrum for analysis. For example, the main area associated with the site effect lies between 540 and 660 nm, corresponding to the 580 hemoglobin peak. By modeling the hemoglobin and removing it from the spectra, we may be able to remove information from the spectra that does not help us discriminate between normal tissue and cancer.

Objective 2. Collection and analysis of new data from breast tissue and axillary nodes.

a) Map excised axillary nodes optically and match the spectra with histology from exactly the same sites.
b) Develop better algorithms for spectral analysis for reliable detection of metastatic cancer in these nodes.
c) Explore the previous anecdotal observation that ESS may detect abnormalities that are not visible on conventional histology, but that are detectable using immunocytochemistry.
d) Collect new data pairs from biopsies taken using the mammotome (vacuum assisted biopsy).

The work under this objective was limited to axillary nodes and will be presented in two major parts. In the first part, only a limited number of spectra were taken from each node (range 4-16), depending on the size of the node. In the second part, nodes were comprehensively scanned at a resolution of 400 spectra per cm^2. When the scanner became available, each node had conventional ESS measurements (up to 16 per node), as used earlier as well as the full scan, so the results could be compared.

During the period from 1st July 2004 – 30th June 2006 we recruited 103 patients to this study. We have expanded our dataset by the addition of 2000 ESS point measurements with matching histology from 130 sentinel and axillary nodes from 90 patients.

In addition, we have performed ESS scanning on 84 nodes from 47 patients. 12 of these nodes underwent repeat scanning (mainly to see if isolated spectra suggesting cancer were reproducible) resulting in a total of 96 ESS scans produced from 38400 spectra. Almost all scanned nodes also had point measurements as made in the earlier part of the program, so the 2 techniques could be compared.

The **new** data set with matched histology consists of:

ESS Point Measurements

Total metastases	12
Partial metastases	40
Micrometastases <2mm	10
IHC detectable submicrometastases <0.2mm	3
Normal nodes	95
TOTAL	**160**

ESS Scanner Measurements

Total metastases	15
Partial metastases	17
Micrometastases <2mm	5
IHC detectable submicrometastases <0.2mm	0
Normal nodes	47
TOTAL	**84**

The majority of the previous data was obtained during an earlier project funded by the USARMC (DAMD17-98-1-8343).

Studies with small numbers of spectra

Currently our total dataset consists of 481 axillary nodes with 4494 spectra matched with histology. This data was collected from 279 patients (including those studied in the previous program and those whose nodes were scanned. The scans are analyzed separately below). The entire dataset now consists of:

	Number of Nodes	**Number of Spectra**
Normal Nodes	356	3091
Micrometastases detectable only with IHC	3	48
Micrometastases (<2mm diameter)	15	202
Partial Metastases (>2mm)	68	721
Total Metastatic Replacement	39	432
TOTAL	***481***	***4494***

The mean number of point measurements from each node is now 9.3 spectra per node (previously 5.6 spectra per node). This is the result of a change in strategy during this programme to increase the surface area sampled by taking 16 point measurement spectra per node, unless the node was very small.

Mean spectra from normal and totally metastatic nodes are plotted below (fig 8). Partially metastatic, micrometastatic and submicrometastatic nodes were excluded from this plot, as the spectra from these groups of nodes consist of a mixed population of positive and negative spectra. This plot shows the fundamental difference between spectra from normal nodes and metastatic nodes. It is re-assuring to note a distinct separation between the normal (blue line) and totally metastatic nodes (red line). This is the difference utilized to make diagnoses from spectra.

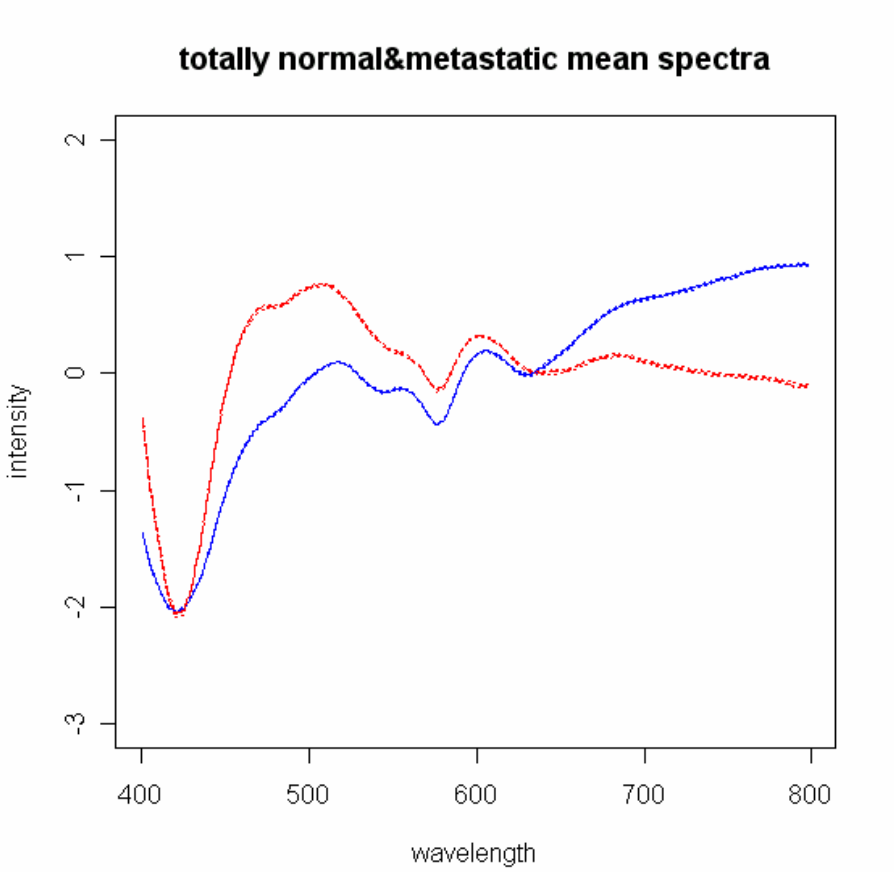

Figure 8. Mean cropped and normalized spectra from normal and metastatic nodes. The blue line is the mean of the normal nodes, and the red line is mean of the totally metastatic nodes.

For analysis a training set was established from 85% of the totally normal and totally metastatic nodes. A discriminant algorithm was developed on this training set by jackknife analysis. A jackknife analysis is computed by developing a linear discriminant algorithm on the entire dataset less one. This algorithm is tested on the spectrum left out. The process is repeated iteratively for each spectrum in the dataset, and the final algorithm developed therefore from the combination of each individual algorithm. A leave-one-out cross validation was performed to test the algorithm on the independent test set of nodes, which consisted of :

- The remaining 15% of totally metastatic nodes and normal nodes
- All subclasses (partial, micrometastatic and submicrometastatic) of incompletely metastatic nodes within the dataset.

The sensitivity and specificity of prediction is shown in table 3 below. It can be seen the algorithm was able to detect totally metastatic nodes with 100% sensitivity, and diagnose normal nodes with 60.4% specificity. Partially metastatic, micrometastatic and submicrometastatic nodes were diagnosed with lower sensitivity.

Table 3 : Summary of results of initial analysis for sensitivity and specificity for detection of cancer on a per node basis, using jackknife analysis using a training set of 85% of totally metastatic and normal nodes

	Sensitivity	**Specificity**
Totally metastatic nodes	100%	
Partially metastatic nodes	54.4%	
Micrometastases (<2mm)	33.3%	
Submicrometastases (<0.2mm)	33.3%	
Normal Nodes		60.4%

The poorer results with nodes that are only partly metastatic are almost certainly due to sampling errors. This is not surprising if only a small percentage of the volume of the node is interrogated, when areas of cancer may be missed. More detailed optical sampling was required to improve sensitivity.

The obvious way forward was to perform more exhaustive ESS sampling of the cut surface of the node by taking spectra from many more sites on each cut surface. This is the approach that we investigated further, and describe below. The other important consideration is to increase the number of surfaces sampled by cutting the node into more slices. It is known that ESS cannot interrogate tissue to a depth of more than about 0.5mm, so to be sure that every point in a node is sampled, it will be necessary to cut nodes into 1mm slices and scan both sides of each slice.

In this program, it was only feasible to undertake the first option – to continue just to bi-valve each node and fully scan one cut surface.

Studies using an ESS scanner

Development of an ESS scanner for intensive optical sampling of tissue.

We have designed and built a prototype device that is able to perform multiple systematic ESS measurements across the cut surface of the node. The device consists of a static standard ESS probe and a mobile X-Y stage, which is moved incrementally across a glass plate on the cut surface of the node. The technical development of the scanner used for this part of the project was undertaken under separate funding from Hamamatsu Photonics. The scanner has been developed in close collaboration with optical engineers from Hamamatsu Photonics and a joint patent application between UCL and the company has been submitted.

Calibration experiments were undertaken to show that spectra taken through the glass plate are comparable to those taken with the ESS probe placed directly on the surface of the node.

Axillary node scanning

Methods

Sentinel nodes were located using the combination of blue dye and radiocolloid and removed for examination. All removed nodes were bivalved. Excised nodes were examined by 3 different techniques – ESS, touch imprint cytology and conventional histology.

Directly after excision, slides for touch imprint cytology (TIC) were prepared from the bivalved cut surface of the nodes, stained with a rapid Giemsa stain and examined immediately by a pathologist. Then, a 1x1cm area of the cut surface of the node was scanned using the ESS scanner. The steps between ESS measurements were set at 0.5mm, hence 400 spectra were measured per cm^2. For small nodes, both cut surfaces were scanned. When nodes were larger than 1cm, a single cut surface or part of a single cut surface was scanned.

After scanning, all nodes were fixed in formalin and sent for conventional histopathological processing. Sentinel nodes were sectioned at a minimum of 3 levels and stained with haematoxylin and eosin (H&E). In addition, nodes with no evidence of metastases on H&E underwent immunohistochemical (IHC) staining for cytokeratin using AE1 and AE3 antibodies.

In patients undergoing axillary clearance, non-sentinel axillary nodes were also available for examination. These were examined histologically with cuts at just one level with H&E staining.

An automated routine for analysis of measured ESS spectra was developed using the GNU-R statistical software package (R Development Core Team, 2005). This consisted of:

1. Spectral pre-processing :
- Smoothing: Using the Savitsky-Golay linear filter
- Cropping from 400nm-800nm : The signal-to-noise ratio above and below this spectral region was low and so uninformative, hence these regions of the spectra were removed prior to further analysis.
- Normalization: By subtraction of the mean and division by the standard deviation, each spectrum has a mean of 0 and a standard deviation of 1. This enabled comparison of spectra of different intensities.
- Data reduction: By "combing" every 7^{th} spectra : This entails extracting every 7^{th} spectra and discarding the intervening spectra, thereby reducing the data by a factor of 7, whilst maintaining the spectral shape.

2. Data analysis:
- Principle component analysis (PCA): To identify spectral features, the first 15 principle components were extracted for analysis (though good discrimination can be achieved from as few as the first 3 PC's).
- Linear discriminant analysis (LDA): A discriminant algorithm was developed from a training set of 2644 ESS point measurements from 308 normal nodes and 34 totally

metastatic nodes. Partially metastatic nodes were excluded from the training set to ensure that all spectra are truly representative of the class (spectra measured from partially metastatic nodes would logically consist of a mixture of normal and metastatic spectra). The training set of spectra was collected over several years (including the period supported by a previous USARMC grant DAMD17-98-1-8343). Note that this is a different algorithm to that developed from the jackknife analysis presented above, which includes point measurements from nodes within the scanner dataset. The algorithm used for analysis of the scanner data was intentionally developed on nodes which were not scanned. This data is therefore *entirely independent* of the test set of spectra acquired using the ESS scanner, enabling the scanner data to be interpreted as a prospective test of the ESS algorithm.

A density plot of the canonical scores determined by jackknife analysis of these 2644 ESS measurements is shown in figure 10. It can be noted that there are two distinct peaks visible, the first at a score of 0, corresponding to normal nodes, and the second just above 4, corresponding to metastatic nodes. Despite the clear peaks, there is some overlap between the 2 classes of nodes between canonical scores of 1 and 4.

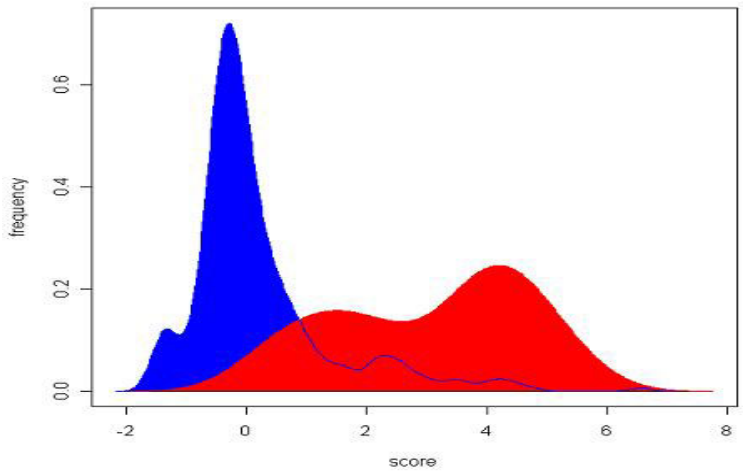

Figure 10. A density plot showing the distribution of the canonical scores of the training set of spectra. Normal nodes are plotted in blue and metastases are plotted in red. The canonical score is plotted on the x axis, and the frequency, as a percentage of the total number in each class is plotted on the y axis.

3. Plotting of ESS Scanner Image:

The output of the LDA is the canonical score. Negative canonical scores indicate spectra likely to be from a normal region of a node and positive canonical scores are spectra likely to be from tumor. Using GNU-R, each spectrum within the 20x20 matrix was plotted on a false color map, with negative canonical scores assigned as blue pixels and positive canonical scores assigned as red pixels. The intensity of each color quantifies the canonical score –

hence areas very likely to be normal are high intensity blue areas on the color map, and areas very likely to be metastases are high intensity red areas on the color map.

The images generated are therefore novel images reflecting areas within nodes likely to be metastases. This technique can be considered an entirely new imaging technique. The images generated were compared to the intraoperative touch imprint cytology and final histology results.

RESULTS & DISCUSSION

The ESS scanner was used to scan 84 axillary nodes from 47 patients. Of the 84 nodes, 72 were sentinel nodes. In addition, scans were performed on an additional 12 axillary nodes from 4 patients undergoing axillary lymph node dissection following a metastatic sentinel node biopsy.

Final histology showed metastases in 37 of the nodes. 47 nodes had no metastases. The breakdown of the extent of metastatic involvement is shown below in table 4.

Table 4 : Table of final histology on Test Nodes

	METASTASES	***NO METASTASES***
Normal nodes		47
Total metastases	15	
Partial metastases	17	
Micro metastases (<2mm)	5	
Isolated tumour cells (<0.2mm)	0	
TOTAL	***37***	***47***

A.

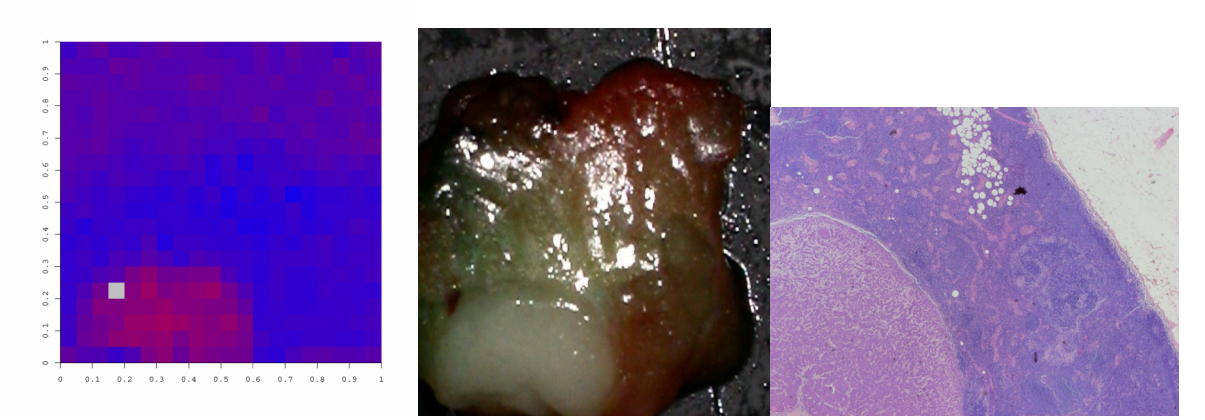

B.

Figure 11 : Representative ESS scans with corresponding photograph and final histology (H&E stain) from a sentinel node with metastases study number SC8471 (A) and without metastases study no SC8523 (B)

Several features can be seen in these images:

1. There is a discreet metastasis measuring 4.7 x 2.7mm in example 11 A, which is visible to the naked eye, and clearly shown as the pink staining area with typical features of a ductal carcinoma on histology. This metastasis shows clearly on the ESS scan as a discreet high intensity red area. The surrounding normal node is blue. This scan is highly illustrative of the ability of ESS scans to differentiate tumour from normal node.

2. The area surrounding the nodal tissue shows as a low intensity red signal, seen in both examples, though more apparent in example 11 B. This is an artefact seen in any scans which have background visible within the area of the scan. This artefact results because linear discriminant analysis is a 2 way classification. The discriminant algorithm has been developed using a training set of cancer metastases and normal lymph nodes. Spectra measured from areas outside the node are more like those from metastases than normal node, and hence have positive canonical scores, and are therefore plotted as red. For ease of further discussion in the report, we will term this "background artefact". For qualitative analysis of ESS scans, these areas should be ignored. Hence, to understand an image, it is important to

match the macroscopic appearance of the node to be scanned with the ESS scan. This can conveniently be done while the node is under the scanner, or by taking a photograph of the node under the glass plate. A more scientific statistical approach to this problem will be discussed later in the report.

3. The ESS scan of the normal node in 11 B has an overall blue appearance with no focal areas of red on the ESS scan, and hence this is a negative scan (no metastases). It can be noted that while the overall impression of the node is blue, there are in fact low intensity pink areas within the node. This can be understood by re-examining figure 10, which is a density plot of the canonical scores of the *training set* of normal nodes (shown in blue) and the metastases (shown in red). Despite selecting only totally normal and totally metastatic nodes for training, there remains some overlap within the scores. The threshold for the color mapping was set at 0. As a consequence, areas of normal nodes may have low intensity red signals within them (as a result of weakly positive canonical scores), and hence are plotted as a low intensity purple coloring. This could be overcome for future analyses by increasing the threshold of the canonical score for assigning color distinction (for example to 4). The second possible conclusion that can be drawn from this plot is that to diagnose metastases, only high intensity red areas, corresponding to canonical scores greater than 2 should be considered.

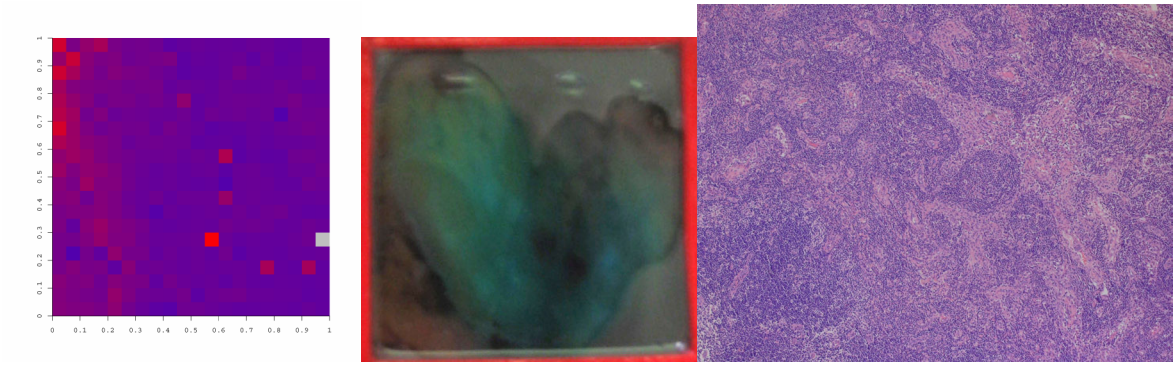

Figure 12 : An ESS scan, macroscopic photograph and final histology from a normal (non metastatic) node, study number SC8431.

A further example of a scanned node which exhibits a different artifact is shown in figure 12. In this example, of a normal (non-metastatic) node there are further features to be noted:

1. On the ESS scan, there is an area with red pixels in the lower left part of the scan. Inspection of the photograph shows this to be an area of perinodal fat. This is a second form of artifact produced on the ESS scans, and happens for a similar reason to the background artifact described in point 1 above. This artifact appears less marked than the background artifact described above. This artifact can be avoided by dissecting the node from the perinodal fat before performing the ESS scan, or by disregarding these areas by correlating the ESS scan with the appearance of the node under the glass plate. Once again, a different statistical approach to this artifact will be discussed later in the report.

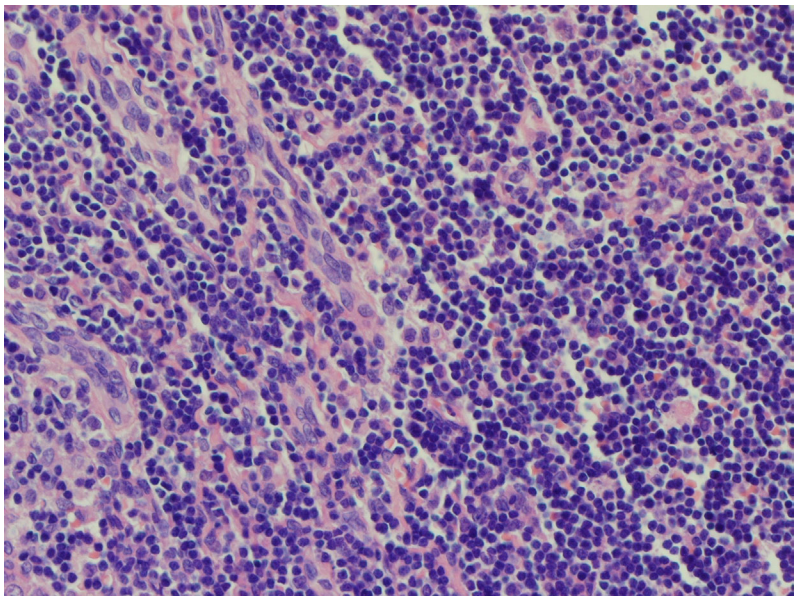

Figure 13 : High power photomicrograph of normal node SC8431 over the area resulting in a high intensity positive pixel on ESS scanning. Towards the left side of this image are pink staining cells with larger nuclei which are normal stromal components of lymph nodes.

2. There are several red pixels within the area representing the substance of the node towards the middle of the scan. The lower intensity pixels may be explained by perinodal fat lying between the 2 halves of the bivalved node. There is however a single high intensity red pixel which appears truly within the nodal tissue. Figure 13 shows a high power view of the histological appearance of this area of the node. Larger cells with pink stained cytoplasm and large nuclei can be noted on the left side of this image. These are stromal cells, which are part of the normal population of cells within a lymph node. This raises the question of whether these stromal cells may account for the high intensity signal within this particular example. An alternative explanation for this single high intensity pixel is that this is an occasional measurement artifact in the ESS spectra. If this was the case, these spectra are likely to be random occurrences, and would not be reproducible if the node was rescanned, or scanned in a different orientation. To elucidate this, ESS scans which showed this artifact were rescanned either at the same 0.5mm resolution or at a higher 0.25mm resolution.

Examples of repeat scans are shown in figure 14. These show that the spectra do indeed appear to change, suggesting that this is a random background phenomenon, possibly due to measurement artifact. There are several ways to tackle this problem:
1. To rescan every node, and only to consider the lowest score at each pixel for diagnosis
2. To scan the node once, but to take several measurements at each pixel, and then consider either the lowest score or an average of the scores for diagnosis
3. To increase the threshold number of pixels for a positive diagnosis. This would increase the specificity of diagnosis, but at the expense of sensitivity. This is the approach we have taken in this analysis, both due to limitations imposed by the software used during this study,

as well as time limitations imposed by the scanner before autolysis of the specimen occurs, thereby interfering with histological diagnosis.

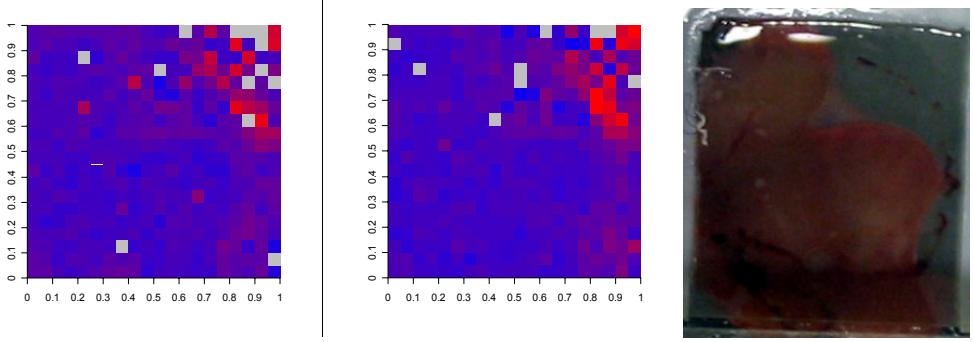

A. SC8892

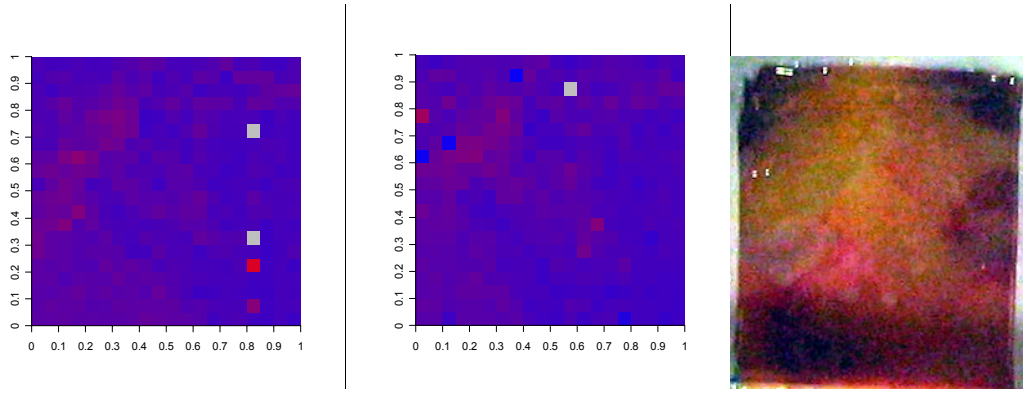

B. SC8872

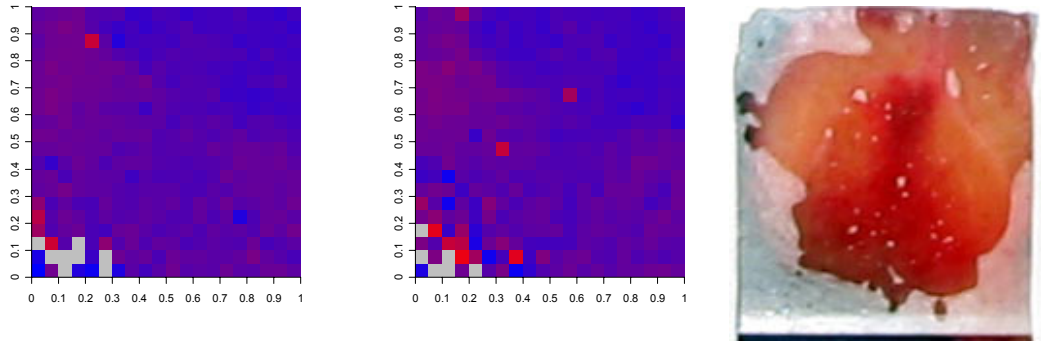

C. SC8861

Figure 14 : Examples of normal (non-metastatic) nodes with high intensity positive pixels, submitted to rescanning. Note that these high intensity positive pixels alter on repeat scanning, suggesting that this misclassification is due to some random effect, postulated to be an artifact of measurement.

The final artifact noted within the series of scans is of grey pixels. The software written to encode the color maps was programmed to record any spectra falling outside 2 standard deviations of the mean of the training set as unclassifiable, and to plot these in grey. 2 examples of these scans are shown in figure 15.

A. SC8461

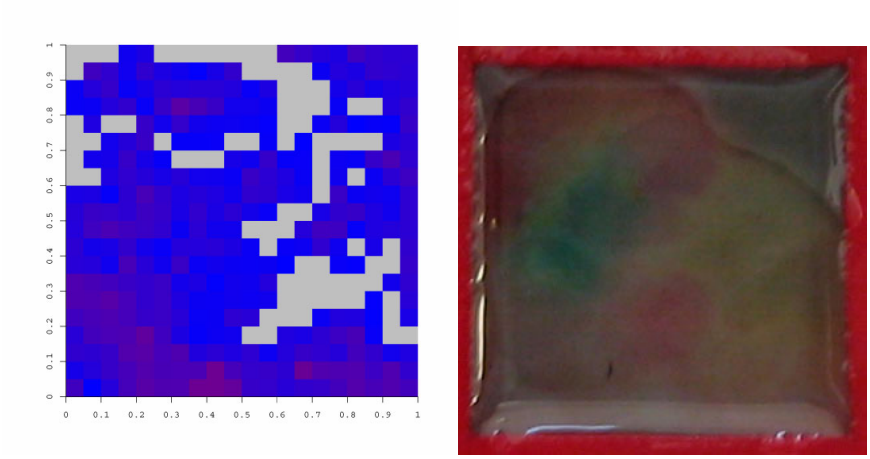

B. SC8982

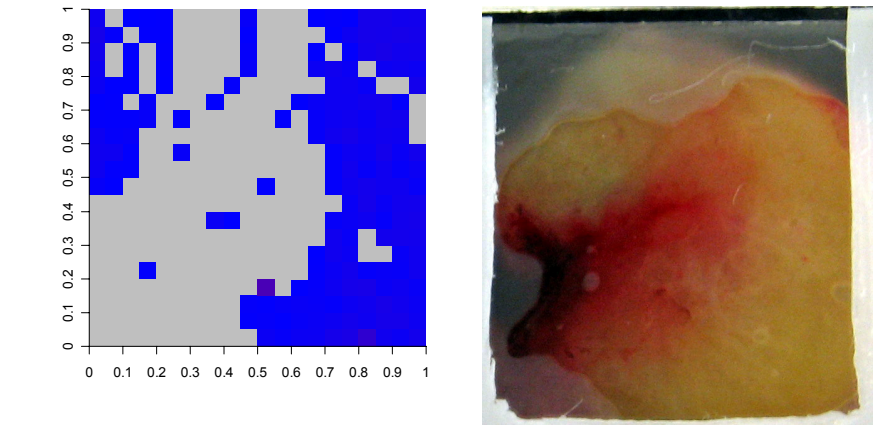

Figure 15 : Unclassifiable spectra are those spectra which fall outside of 2 standard deviations of the spectra within the training set and are plotted as grey pixels. Example A shows grey areas within the scan which represent saturated spectra. Example B is from a patient who underwent preoperative (neoadjuvant) chemotherapy, and who was found to have fibrosis within the sentinel nodes on histological examination.

In the first example 15 A, the number of pulses of light has been set too high resulting in saturated spectra. This particular scan was performed early within the series whilst the methodology was under development. Saturated spectra can easily be recognized by the user, and corrected for by reducing the number of pulses of light delivered to the illumination fibre. An alternative solution is to incorporate an "autoranging algorithm", which immediately

analyzes measured spectra, and automatically adjusts the number of pulses of light according to the measured spectra. In this way, the highest possible signal-to-noise ratio can be achieved, without the risk of saturation. The autoranging algorithm proved difficult to develop and deploy and was only made satisfactory near the end of the project, so has not been used to collect any of the data presented in this report.

In the second example 15 B, the number of pulses was correctly set, but despite this, many unclassifiable spectra were measured. These grey pixels were consistently present on a repeat scan of this node, and interestingly, a similar pattern was noted in a second node scanned from the same patient. This particular patient had undergone pre-operative (neoadjuvant) chemotherapy. The primary tumour had responded well to this chemotherapy by the time surgery was performed. Histological examination of the nodes showed complete regression of axillary node metastases but with fibrosis evident, possibly as an effect or chemotherapy or as a result of regression of nodal metastases following chemotherapy. It is postulated that this is the reason the system was unable to classify the majority of spectra from this patient, as the training algorithm was developed on normal nodes and metastases only. This issue warrants further study in the future.

Evaluation of the Accuracy of Diagnosis of Sentinel Node Metastases by ESS Scanning

To evaluate the overall accuracy of diagnosis of sentinel node metastases, all images were examined by a single investigator. The principles used for interpretation of the images were:

1. Pixels lying outside the node and within perinodal fat were ignored
2. Where nodes underwent more than one scan, the observer was able to consider the results from all scans
3. The number of high intensity red pixels was counted and recorded by the investigator. Any more than 10 positive pixels were recorded as >10.

7 nodes from the dataset were excluded from the analysis for technical reasons: 2 due to incorrect calibration of the device, 2 due to saturated spectra due to setting the number of pulses too high by the operator, 1 due to mechanical failure of the device and 2 due to unassessable scans as a result of fibrosis in the lymph nodes.

Empirical and fitted receiver operator curves (ROC curves) were generated using JROCFIT 1.0.2 and JLABROC4 (John Hopkins University, Baltimore, USA). The final histology of the node was used as the gold standard for diagnosis. The ROC curves of the initial analysis are shown in figures 16 and 17. The 11 points on the empirical curve represent the accuracy from 0 positive spectra on the right hand side of the plot sequentially to >=10 positive spectra on the left side of the plot.

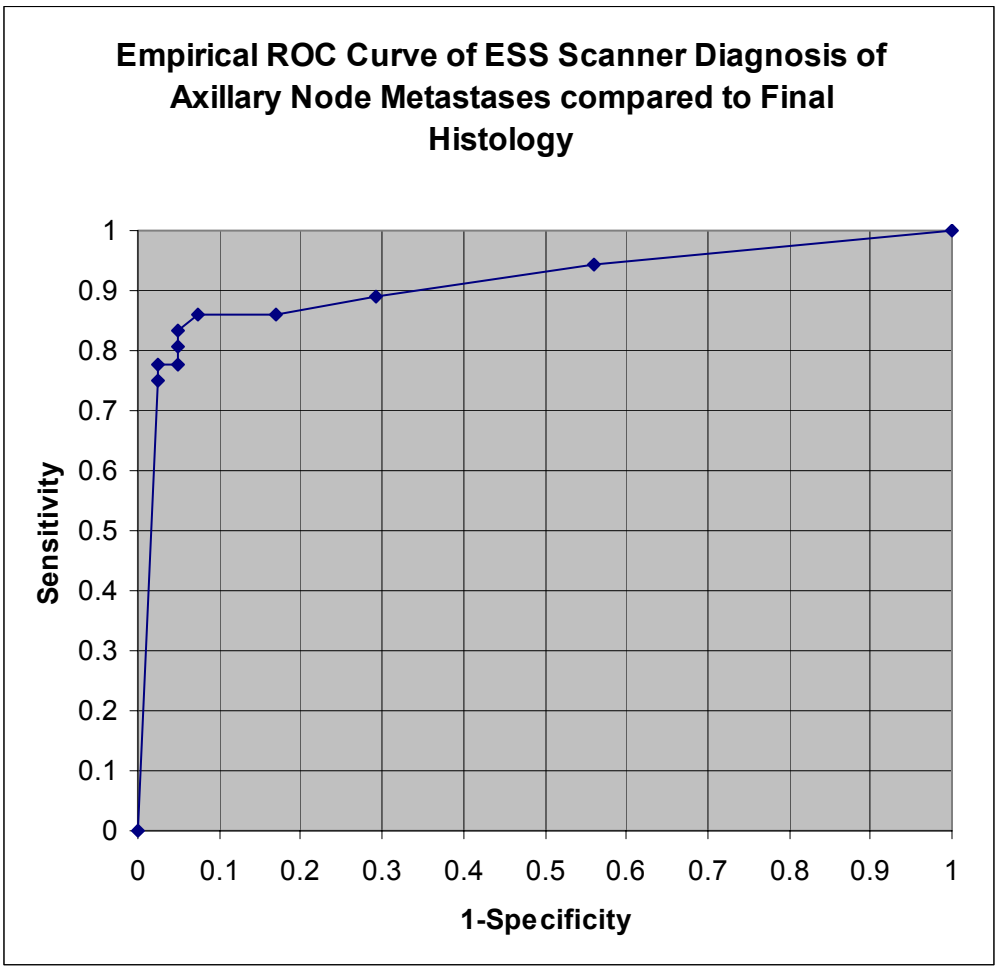

Figure 16 : Empirical ROC curve of accuracy of diagnosis of axillary node metastases using ESS scanning vs. *final histology. The area under the curve is 91.2%.*

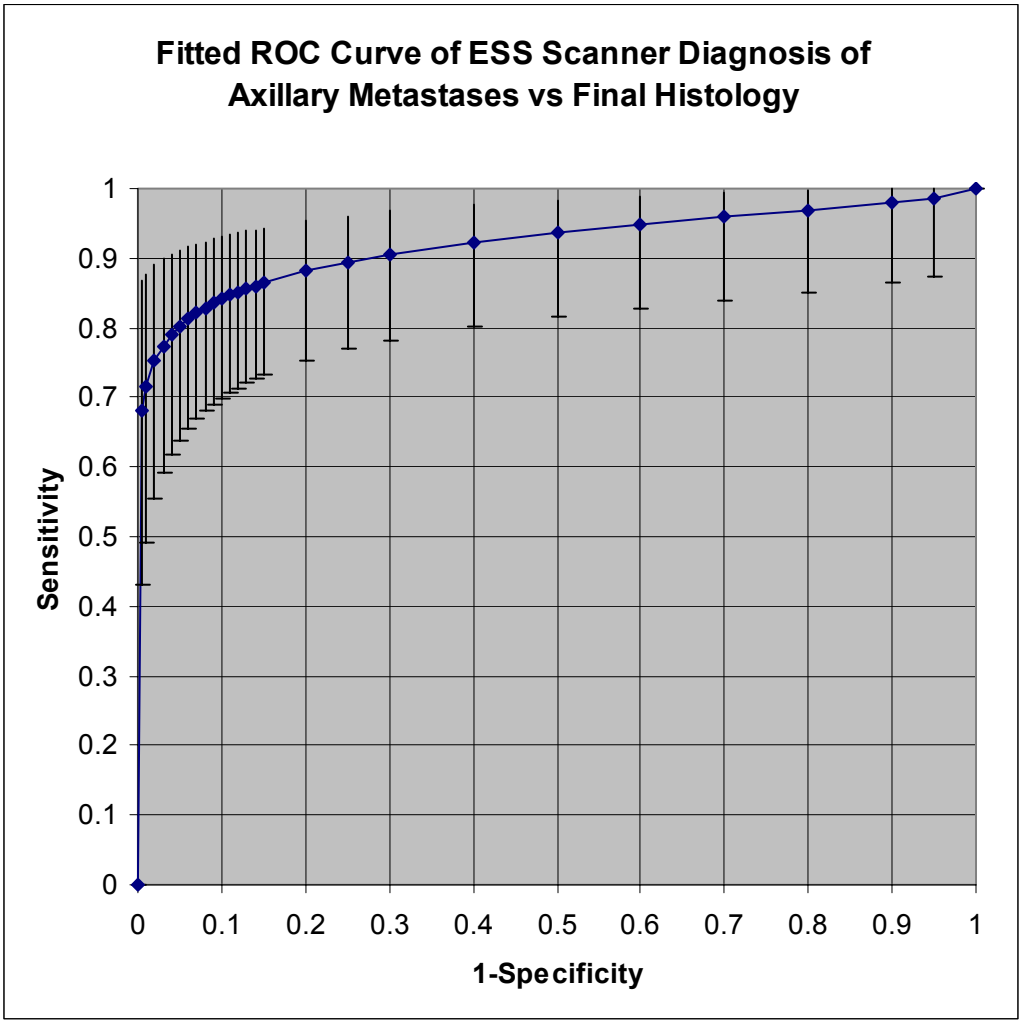

Figure 17: Fitted ROC curve of accuracy of diagnosis of axillary node metastases using ESS scanning vs. *final histology. The error bars represent the 95% confidence interval of the plots. The area under the curve is 92.1%.*

Examination of the empirical ROC curve shows accuracy is maximal using a threshold of 5 pixels for diagnosis, which gives a sensitivity of 83.3% and a specificity of 95.1%. For this particular application, high specificity of diagnosis is required, to avoid the surgeon performing an unnecessary therapeutic axillary lymph node dissection based on a false positive result. This would negate the main purpose of performing sentinel node biopsy, which is to avoid the morbidity of axillary dissection in patients with no metastases within the sentinel node. Specificity can be improved at the expense of sensitivity by shifting the threshold for diagnosis to the left.

If we consider the point where 8 positive pixels are required for a positive diagnosis, the sensitivity drops to 77.8% but the false positive rate halves, and specificity rises to 97.5%. This is considered sufficient specificity of diagnosis for clinical use by the surgical

oncologists at our unit. Sensitivity at this threshold remains comparable to that achieved by existing pathological techniques for intraoperative diagnosis of sentinel node metastases such as touch imprint cytology and frozen section. Indeed this exceeds the sensitivity achieved by touch imprint cytology in this particular series.

A limitation of our current methodology for ESS scanning is that only a single cut surface of the lymph node is examined. This becomes relevant when considering patients with small metastases. It is conceivable that a small metastasis may be deeper than the cut surface of the lymph node, and hence not be detectable using ESS scanning. This point is illustrated in figure 18. Previous work done by ourselves on touch imprint cytology has demonstrated that the majority of false negative touch imprint cytology diagnoses are due to sampling rather than interpretation failures. A similar principle can be applied to ESS scanning. Whilst in theory, ESS may detect lesions up to about 0.5mm below the tissue surface, in practice, we consider that it will probably be difficult to detect metastases that are not present on the cut surface of the node. This similarity between ESS scanning and touch imprint cytology is the basis for the next analysis.

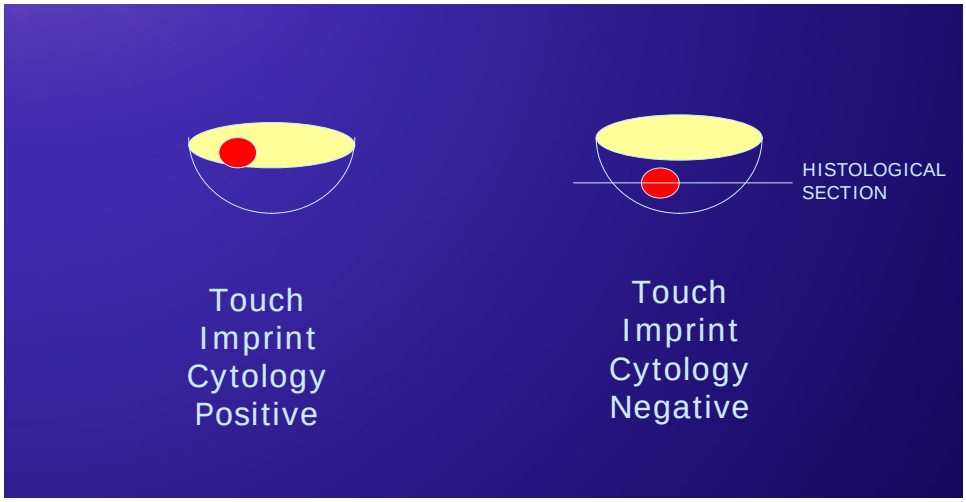

Figure 18 : An illustration of the effect of small metastases lying deeper within the substance of the node. These may fail to be detected by ESS as well as touch imprint cytology, though detected later on final histology which is performed at multiple levels.

Within the dataset, there are 7 nodes with false negative diagnoses on touch imprint cytology. We make the assumption that this is due to the tumour lying deeper than the cut surface of the node. These 7 nodes were therefore excluded from the dataset for this second analysis. Included within these 7 nodes was 1 node that was positive, and hence correctly diagnosed on ESS scanning. The rationale for the second analysis is that by excluding nodes where the tumour is assumed to be deeper than the cut surface, we get a better idea of the true system performance of the ESS scanner. The ROC curves for this analysis are shown in figure 19 and 20.

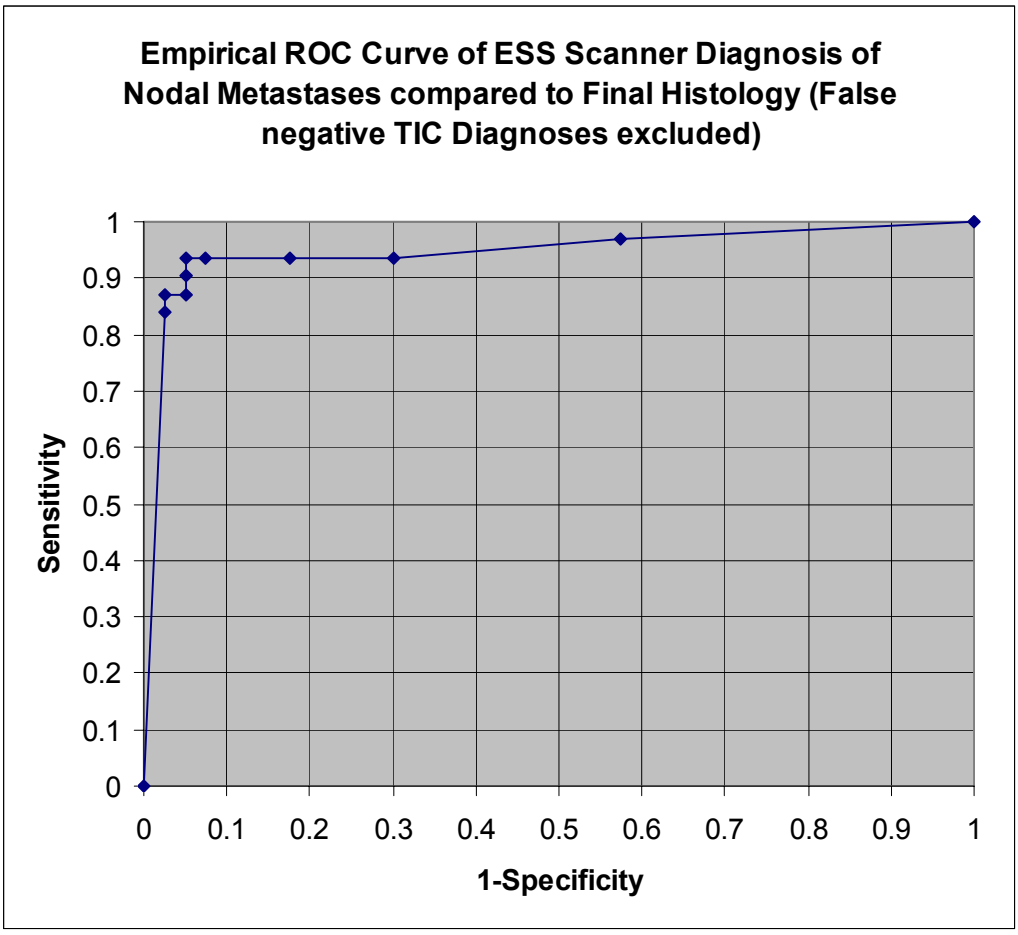

Figure 19: Empirical ROC curve of accuracy of diagnosis of sentinel node metastases with nodes falsely negative on touch imprint cytology excluded.

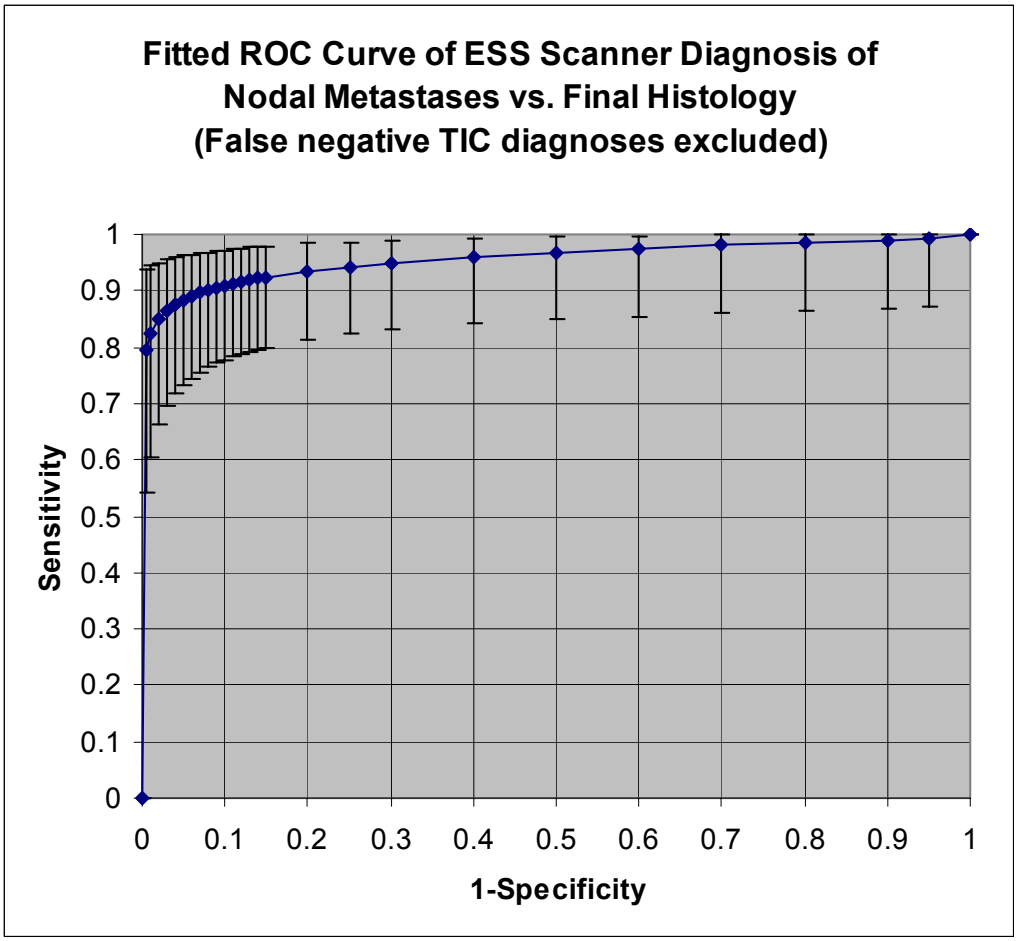

Figure 20: Fitted ROC curve of accuracy of diagnosis of sentinel node metastases with nodes falsely negative on touch imprint cytology excluded. The error bars show the 95% confidence interval.

Examination of the empirical ROC curve shows enhanced sensitivity and as expected unchanged specificity. At a threshold of 8 positive pixels, sensitivity is 87.1% and specificity remains 97.5%.

There are several possible explanations for false negative diagnoses on this analysis :
1. All scans are of a 1x1cm area of the node. As the cut surface of some nodes exceeded the area we were able to scan, it is conceivable that the metastasis lay outside the area scanned.
2. Technical problems with calibration and suboptimal signal to noise ratio, particularly in early measurements may have resulted in technically imperfect scans.

We have addressed some of these issues:
The area we are able to scan has been limited somewhat by the speed of scanning of the prototype device. The prototype scanner was constructed purely to test whether enhanced sampling enhances accuracy, and speed of scanning was not an initial aim. For these initial experiments, a 1 cm^2 scan took 40 minutes. There are obvious benefits to increasing the speed of scanning. We have recently been able to reduce this to 12 minutes by making

software adjustments. Further improvement in scanning speed may be achieved by upgrading the motors moving the stage and will allow larger surface areas to be scanned. In the longer term, our discussion with the optical engineers from Hamamatsu Photonics has raised the possibility of other technical solutions for making scanning faster.

Incorporation of the newly developed autoranging algorithm may improve the spectral quality.

Despite these limitations, the system yields impressive results, which are well within the thresholds needed for clinical use of the device.

Direct Comparison of Touch Imprint Cytology Diagnosis with ESS Scan Diagnosis

Touch imprint cytology is an established technique for rapid diagnosis, and is the intraoperative diagnostic test currently used at our institution. We have shown similar results are achieved to frozen section in our hands(4). This analysis compares the results of ESS scanning with touch imprint cytology.

For this analysis, the results from all 62 nodes with both touch imprint cytology results and technically satisfactory ESS scans were compared. The accuracy of diagnosis of both modalities is compared in table 4 below. The threshold used for a positive ESS scan diagnosis was 8 positive high intensity pixels.

The touch imprint cytology results are reported in Table 5. The overall sensitivity of TIC in this sample was 68%, the specificity was 100%, the positive predictive value was 100% and the negative predictive value 84.6%. Table 6 shows the accuracy of diagnosis of TIC, broken down by the extent of metastatic involvement. It is apparent that TIC performs poorly for micrometastatic nodes, and failed to diagnose any of the 4 micrometastatic nodes within this dataset.

Table 5 : Table of Results of Touch Imprint Cytology on Test Nodes compared to Final Histology

True Negative	44
False Negative	8
True Positive	17
False Positive	0
TOTAL	69

Table 6 : Table of Accuracy of Diagnosis of Sentinel Node Metastases by TIC, broken down by extent of metastatic involvement. TN = True negative, FP = false positive, TP = true positive, FN = false negative

	TN	FP	TP	FN	***Sensitivity of Diagnosis***	***Specificity of Diagnosis***
Normal nodes	44	0				100%
Total metastases			7	1	87.5%	
Partial metastases			10	3	83.3%	
Micro metastases (<2mm)			0	4	0%	
Isolated tumour cells (<0.2mm)			0	0	N/A	
Overall Accuracy	***44***	***0***	***17***	***8***	***68%***	***100%***

Table 7 : Direct comparison of the accuracy of diagnosis of sentinel node metastases by Touch Imprint Cytology and ESS scanning for 62 sentinel nodes

	Touch Imprint Cytology	ESS Scanning
True Negative	38	37
False Negative	8	8
True Positive	16	16
False Positive	0	1
Sensitivity	66.7%	66.7%
Specificity	100%	97.4%
Positive predictive value	100%	94.1%
Negative predictive value	82.6%	82.2%

TIC and ESS scanning achieved the same sensitivity in this direct comparison. A single false positive diagnosis occurred from ESS scanning, resulting in a specificity of 97.4% and a positive predictive value of 94.1% (compared to perfect specificity and positive predictive value by TIC). TIC gave a marginally higher negative predictive value of 82.6%, compared to 82.2%. Accurate TIC diagnosis, of course, relies slide preparation and staining and on the presence of an experienced cytopathologist, whilst ESS scanning does not.

Refinements of scan analysis

We need to validate whether examination of the images by different observers gives consistent results. Whilst criteria for analysis of images were set, there is bound to be some variation in interpretation by observers. An ideal test would remove this subjective analysis of images, and perhaps present the surgeon with a simple "Metastatic or non-metastatic" answer, or report the probability of an individual node of having metastases. To achieve this, some form of quantitative analysis of the matrix of spectra is required.

The qualitative analysis of the images does give useful insight into the data, which can be incorporated into quantitative analysis. An example of this is the recognition that areas outside the node and perinodal fat result in false positive spectra. For quantitative analysis, only spectra actually measured from the node are relevant. For this initial work, these spectra have been manually removed, after identifying them using the photographic images and ESS scans.

The qualitative output from the LDA is the canonical score, which relates to the probability of an individual spectrum appearing normal or metastatic. The distribution of the canonical scores may be a useful tool for identification of metastatic nodes. Figure 21 shows 3 examples: a normal node, a partially metastatic node and a totally metastatic node, with histograms showing the frequency of the canonical scores.

A SC8523 – Normal node

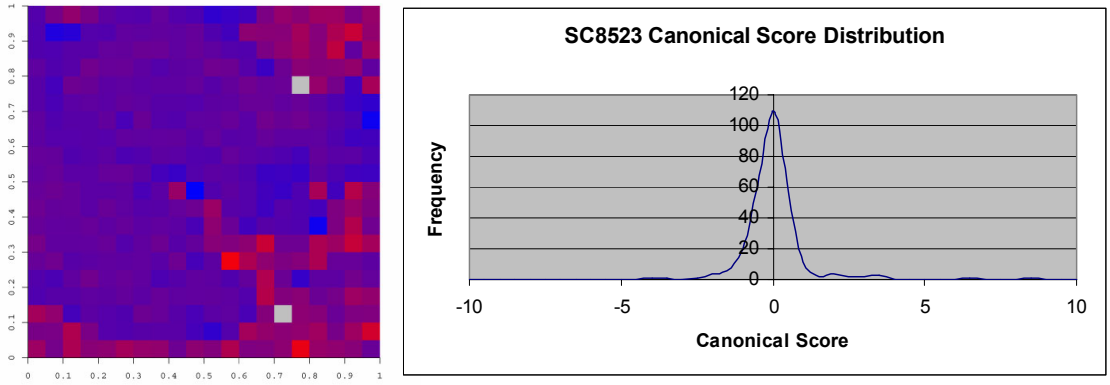

B SC8471 – Partially metastatic node

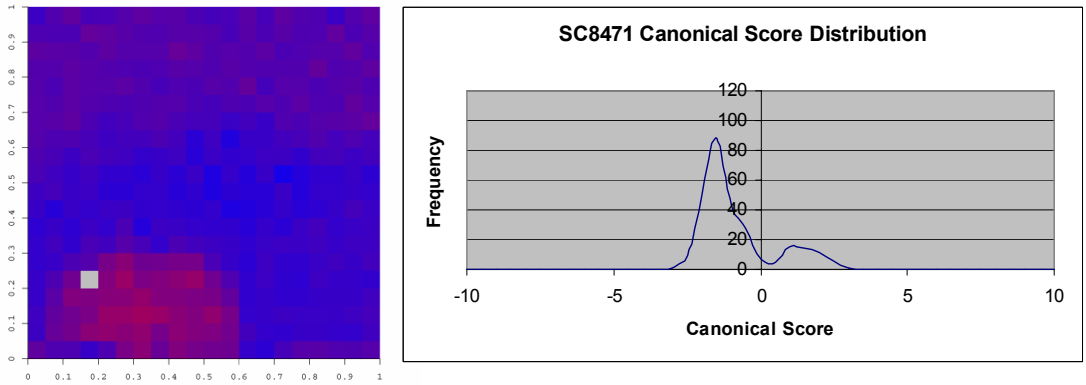

C SC8463 – Totally metastatic node

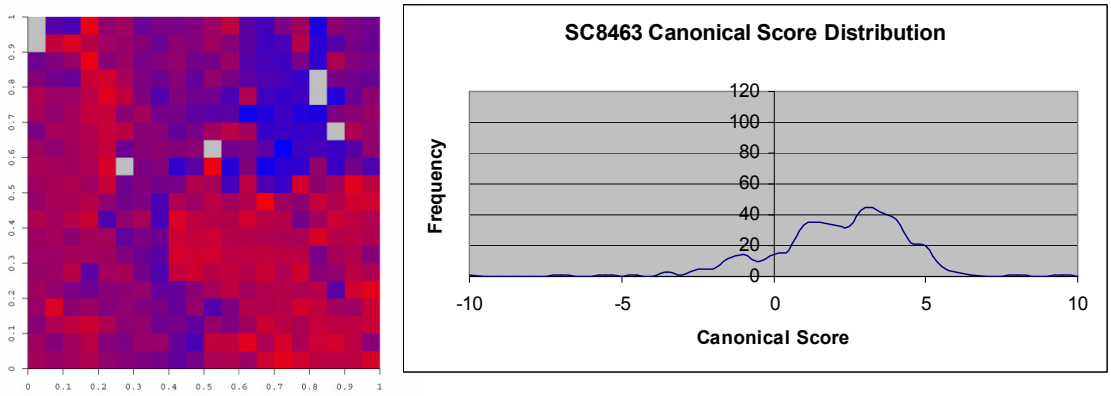

Figure 21: ESS scans and corresponding histograms showing the distribution of the canonical scores for each scan. Spectra outside the actual node have been manually removed for these examples. Example A is a normal (non-metastatic node), example B is a partially metastatic node, and example C is a node completely replaced with tumour.

Examination of these plots shows a pattern emerging:

1. There is a bimodal distribution of canonical scores: The peak on the left hand side of the plot appears to correspond to normal node tissue, and to the right of the plot corresponds to the presence of metastases.
2. There are several possible parameters that may correlate with the presence of metastases, such as the height of the second peak, or the area under the curve of the second peak
3. The qualitative analysis of images shows that high canonical score pixels are more likely to be malignant areas. Application of a weighting factor to increase the relative significance of high canonical scores may be required to define a threshold for diagnosis. An example of such a weighting factor would be using the square of the canonical score.

More work needs to be done before firm conclusions from quantitative analysis of ESS scans can be drawn.

Development of an algorithm for differentiating lymph node from background

Linear discriminant analysis is a binary classification method. The linear discriminant algorithm used for all analyses so far has been developed on ESS spectra measured from normal nodes and metastatic nodes. Application of this algorithm to lymph node scans therefore results in false positive signals from the area surrounding the node.

We have investigated the possibility of developing a separate algorithm able to differentiate the node from the surrounding background. We developed the algorithm using spectra measured from both normal and metastatic nodes, and spectra measured from the surrounding background. The background spectra were collected both from actual scans and experimentally derived by performing scans of the background only. We have tested this algorithm on some of the test set of nodes. Examples are shown in figure 22.

The utility of this algorithm is:
- It will enable enhanced image generation by incorporation of this algorithm prior to applying the normal node vs. metastases algorithm. Thus, only relevant spectra actually measured from nodes are tested by the normal vs. metastatic node. This would avoid the false positive signals from the area surrounding the node – making ANY high intensity red pixels relevant. This would remove the need for correlation of the ESS scan image with the macroscopic appearance, remove some of the subjectivity from interpretation of images and enhance interpretation.
- It will enable more quantitative analysis of spectra from scans, for example in the manner described in the section above. This would facilitate computer based automated analysis of ESS scans, giving a quantitative measure of the probability of a node being metastatic or not. This is preferable to providing an image for interpretation by the surgeon in the high-pressure operating theatre environment.

A similar method is being used to detect the perinodal fat, which would have similar applications.

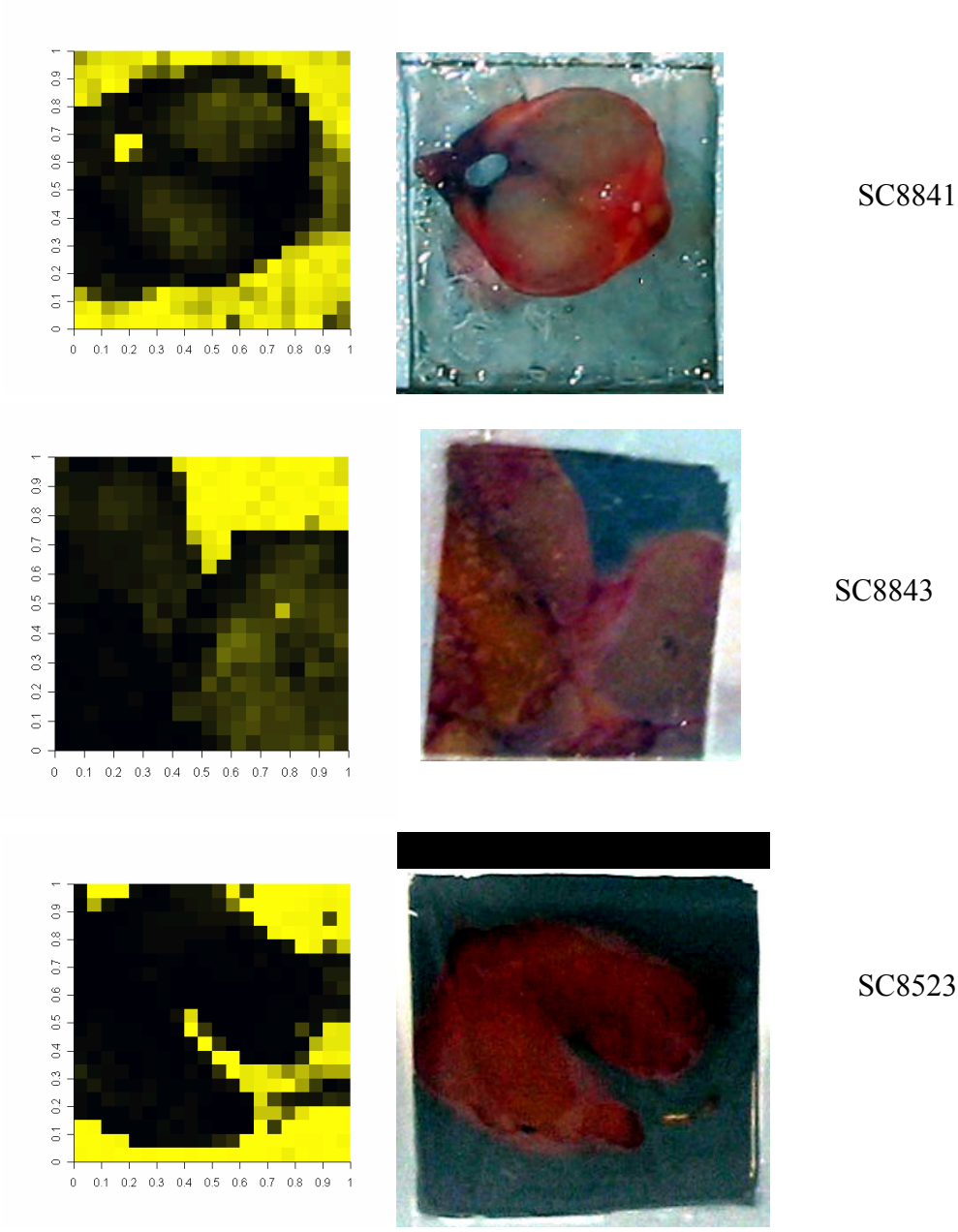

Figure 22: Testing of an algorithm for differentiation of background from node on ESS scanning. The background is plotted in yellow, and remaining node plotted in black.

CONCLUSIONS OF AXILLARY NODE ANALYSES

1. ESS point measurements are able to differentiate between normal lymph nodes and metastatic lymph nodes. The limitation of using point measurements is inadequate sampling of the tissue under examination. This can be largely overcome using the scanning technique described here and by appropriate preparation of the tissue to be assessed so that all layers are adequately assessed.
2. ESS scanning is a completely new imaging technique with the potential for rapid imaging of nodes within 12 minutes. It is capable of detecting breast cancer metastases with similar accuracy to existing techniques used by pathologists, but without the need for interpretation by a pathologist.
3. We have demonstrated that quantitative diagnosis using the enhanced spectral measurements is possible, and have progressed towards this, although there is potential for further development of the analytic techniques used on the current data set.
4. The technique of ESS scanning is essentially ready for further prospective assessment in clinical trials.

Other aspects of objective 2

It was proposed to explore the previous anecdotal observation that ESS may detect abnormalities that are not visible on conventional histology, but that are detectable using immunocytochemistry.

We did not have enough nodes in this category to study this aspect.

Proposed studies on Mammotome Biopsies

The plan in the original statement of work was to also collect spectra from guided mammotome biopsies. Unfortunately, the institution's mammotome biopsy unit is not currently functional, due to the inability to recruit a technician to operate the device. All patients for mammotome biopsies are currently being referred to another unit. This aspect of the project had to be suspended.

Stop Press : Additional data on 2 cases showing detection of low volume metastases by ESS Scanning

We present 2 anecdotal cases, where ESS scanning apparently detects low volume disease within the sentinel node, undetected on touch imprint cytology.

The initial case (SC8921) is included in the series analyzed for the report. The second case, (SC9011) histological analysis was only completed this week, and is not included in the series already analyzed.

Figure S1 shows a photograph of node SC8921 under the scanner glass plate, and 2 corresponding ESS scans at a resolution of 0.5mm per step performed 40 minutes apart, but without changing the position of the node under the plate. The area of the scan representing the node is circled in yellow for clarity. Examination of ESS scan shows consistent high intensity red pixels within the node. There are clearly much more than 8 high intensity red pixels within the node, so our criteria for diagnosis of a metastatic ESS scan are met.

Intraoperative touch imprint cytology was reported as "no metastases" by the cytopathologist. Subsequent review of the touch imprints confirmed this diagnosis. Figure S2 shows a low power and high power photomicrograph of the final histology of a single cut face of the node, stained with haematoxylin and eosin. A pale pink staining area can be seen, even on the low power view. This measures 2mm in maximum dimensions. High power shows this is metastatic ductal carcinoma. This metastasis was seen on 2 out of the 3 histological sections, cut approximately 100 microns apart.

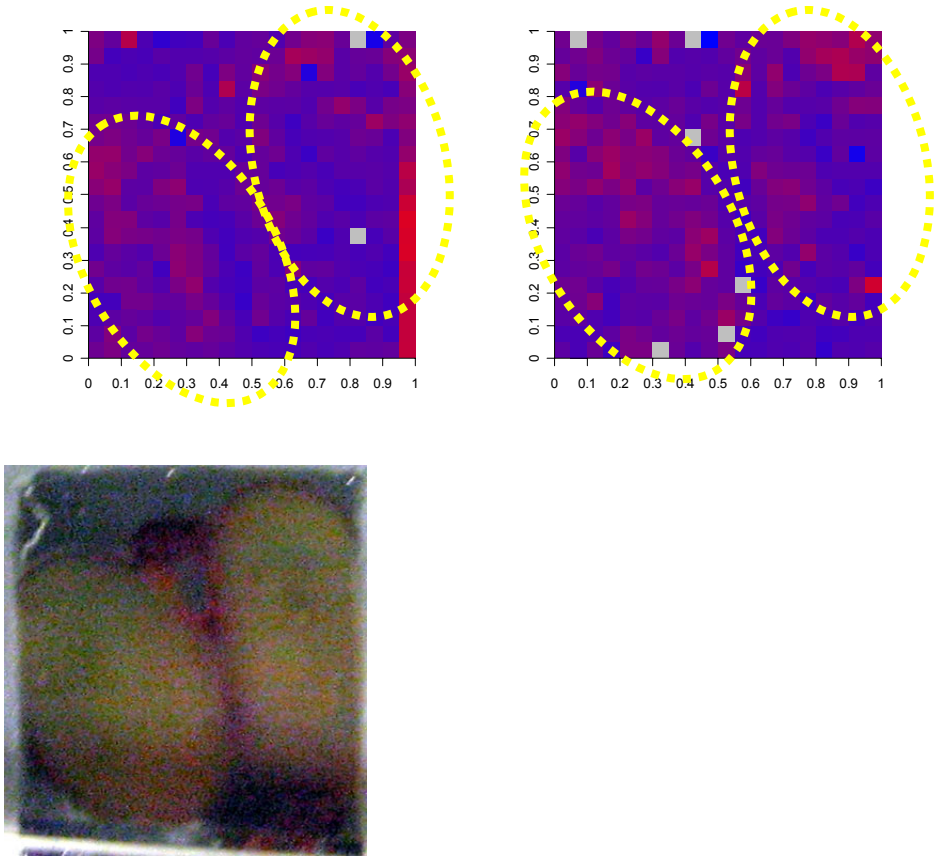

Figure S1 : Photograph and corresponding 2 different ESS scans of node SC8921. The area of the scan circled in yellow is the scan of the actual node (as opposed to the background).

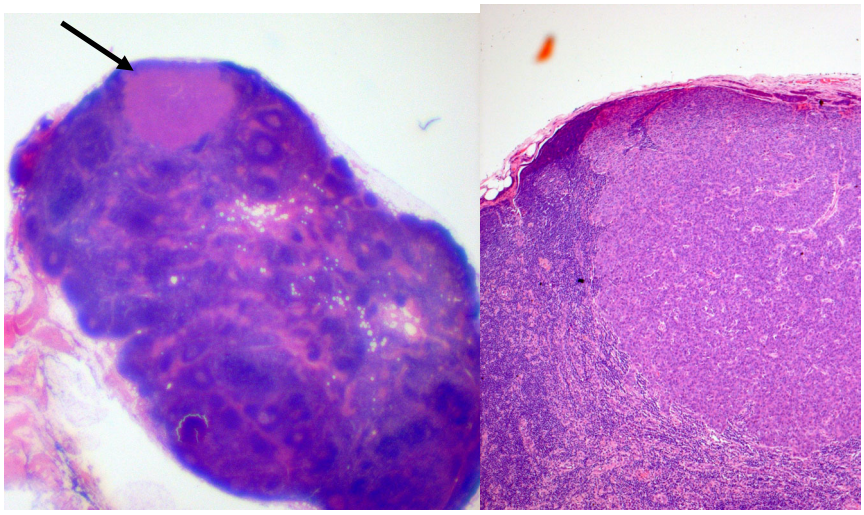

Figure S2 : Final histology of a single surface of node SC8921 stained with H&E. A low power view on the left shows a discreet metastasis (arrowed) measuring 2mm. High power view on right confirms this.

The second case differs slightly. 2 ESS scans are shown in figure S3. This particular node was large, and filled the entire area of the initial ESS scan. The initial scan shown on the left is of a 10x10mm area of the node and was performed with 0.5mm steps. There are 2 areas of high intensity red pixels : in the top left of the scan, and a less prominent area in the bottom right of the scan. The linear red area on the right side of the scan is the plastic spacer at the edge of the scan, and should be ignored. A high resolution ESS scan with a step size of 0.25mm was performed over a 5x5mm area of the node in the top left corner, which is highlighted by the yellow dotted lines in the picture. Examination of this high resolution scan shows a discreet area of high intensity red pixels, suspicious of metastatic tumour.

Intraoperative touch imprint cytology was reported as “no metastatic tumour”. A similar report was issued after review. Final histology is shown in figure S4. On H&E staining, there is tumour noted within the afferent lymphatic vessels lying within the capsule of the node, but no obvious tumour within the node itself. Immunohistochemical staining confirmed tumour within the afferent lymphatics, and scattered clusters of tumour cells within the subcapsular sinus and co-adjacent lymph node. The final histological diagnosis was of submicrometastases/isolated tumour cells

Whilst the criterion of 8 positive pixels on ESS scanning was met, this was only within the high resolution image.

These 2 cases raise the possibility, though are not conclusive evidence that ESS scanning may have the ability to detect low volume metastatic disease, when performed at an appropriate resolution.

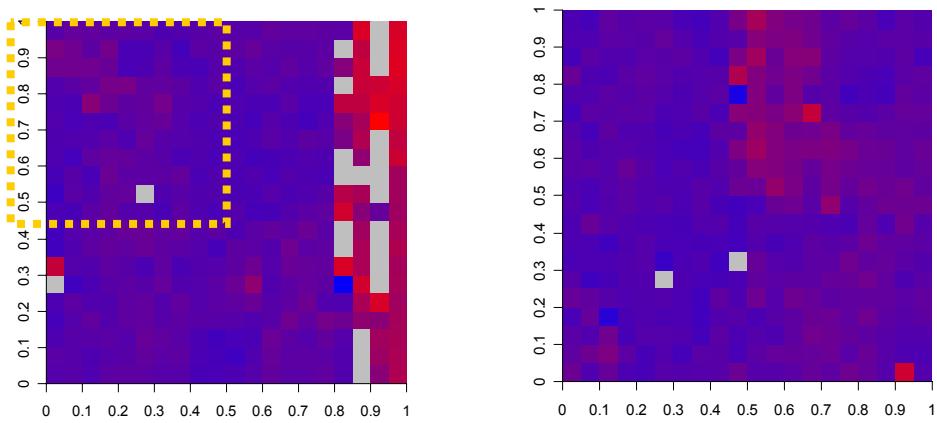

Figure S3 : 2 ESS scans of sentinel node SC9011. The scan on the left was performed with steps 0.5mm apart, and the scan on the right is a higher resolution scan with steps 0.25mm apart of the top left part indicated by the yellow dotted line.

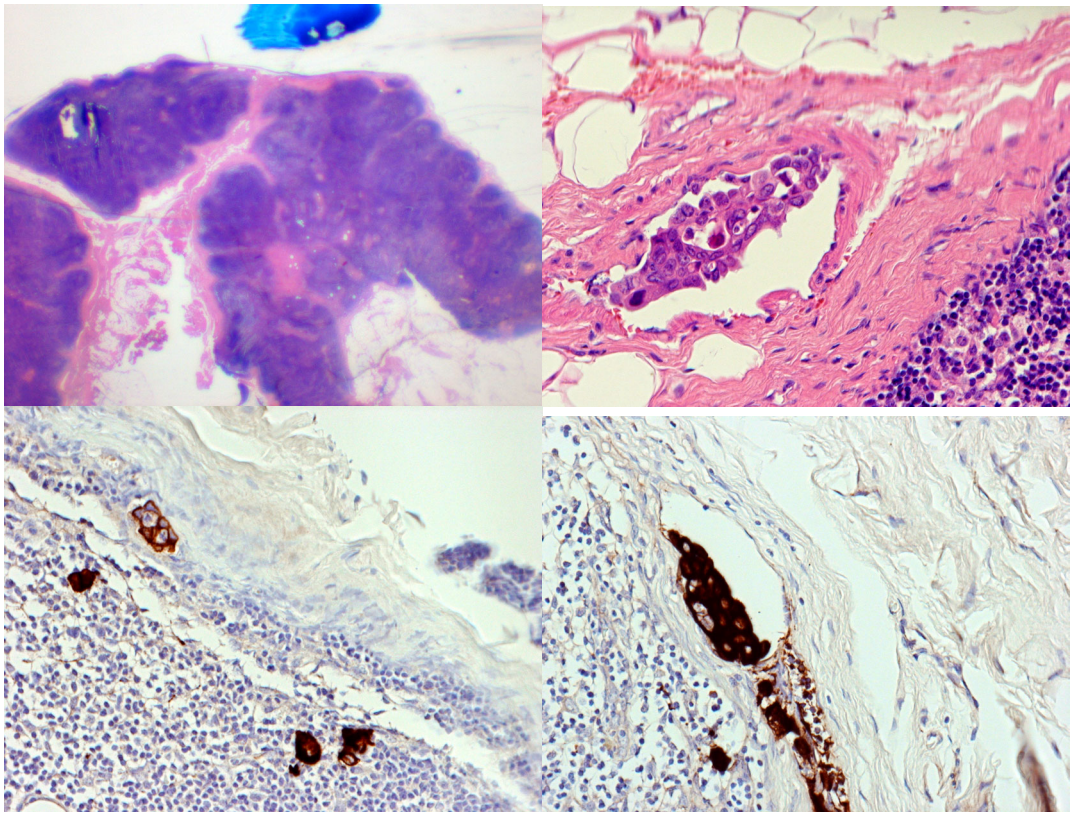

Figure S4 : Final histology of node SC9011. A low power H&E view (top left) shows no obvious sign of metastases. On high power (top right) in the area adjacent to the ink mark, tumour is seen within the afferent lymphatics. Immunohistochemical staining for cytokeratins (bottom) confirms multiple clusters of isolated tumour cells within the subcapsular sinus and nodal tissue

.

Objective 3. Testing the ability of ESS to detect aneuploidy.

a) Take ESS measurements on normal and cancer tissue using the specialized optical probes and match these with conventional histology and standard laboratory techniques for assessing aneuploidy.
b) Using the results from the in vitro work for guidance, develop algorithms for detecting aneuploidy in human tissue
c) If ESS can detect aneuploidy in formalin fixed tissue, to test library breast tissue from patients treated in the past to see if aneuploidy status at the time of diagnosis of breast cancer or DCIS can be used as a prognostic indicator and be correlated with the recent clinical history of the patient

In recent years there has been much interest in developing molecular and cytogenetic markers of prognosis in breast cancer. Reliable markers of prognosis facilitate identification of patients at high risk of systemic metastases, to enable administration of adjuvant systemic therapy (chemotherapy).

Aneuploidy is one such potential marker of prognosis. Aneuploidy is abnormal DNA content (any variation from the normal diploid number of chromosomes). At certain wavelengths, the most significant contribution to the ESS spectra is scattering from cell organelles, particularly the nucleus. Alterations in chromatin content, as occurs in aneuploidy, give rise to localized changes in refractive index of subcellular components, which change the ESS spectra. Recent experiments by our collaborators, and others, have shown that ESS spectra can detect alterations in cellular chromosomal content ex-vivo, a phenonomen closely related to aneuploidy.

We have established a laboratory reference procedure for detection of aneuploidy, using an automated image cytometer (Fairfield imaging, Nottingham, UK). The image cytometer was purchased by the Department of Histopathology for other projects. That department has also appointed a research pathology technician who is able to process specimens routinely for this and other projects. Teething problems with methodology have been resolved and 10 archived breast tumors were initially analyzed as a test series, with satisfactory DNA histograms obtained.

Initially we planned to collect fresh tumour specimens for the study, aiming to take ESS measurement both before and after formalin fixation. In practice, the pathologist found that taking these samples from fresh tumours made margin determination difficult, due to distortion of the tumour when undergoing formalin fixation. We therefore modified our protocol such that spectra were measured only from formalin fixed (as opposed to fresh) tissue to facilitate recruitment. This remains a useful study, as if successful, in practice ESS would be used as a laboratory tool on formalin fixed tissue.

Since modification of the protocol we have been able to recruit 14 patients to the ploidy study so far. One patient had bilateral breast cancer; hence 15 tumours have been analyzed. Large tumors were divided into smaller blocks, and ploidy determined in each block (The ploidy

status may not necessarily be the same throughout any one tumor). We have 42 blocks of tumour samples for analysis. We have ploidy histograms on 22 samples so far – 9 from diploid samples and 13 from aneuploid samples. We have yet to complete image cytometry on 20 blocks of tumour.

Representative example DNA histograms from diploid and aneuploid tumours are shown in figure 23. In the top example, there is a single peak in the integrated optical density at 2C, indicating that this is a diploid tumour. In the bottom example, in addition to the diploid peak at 2C, there is an additional peak at 4C, which is the aneuploid peak.

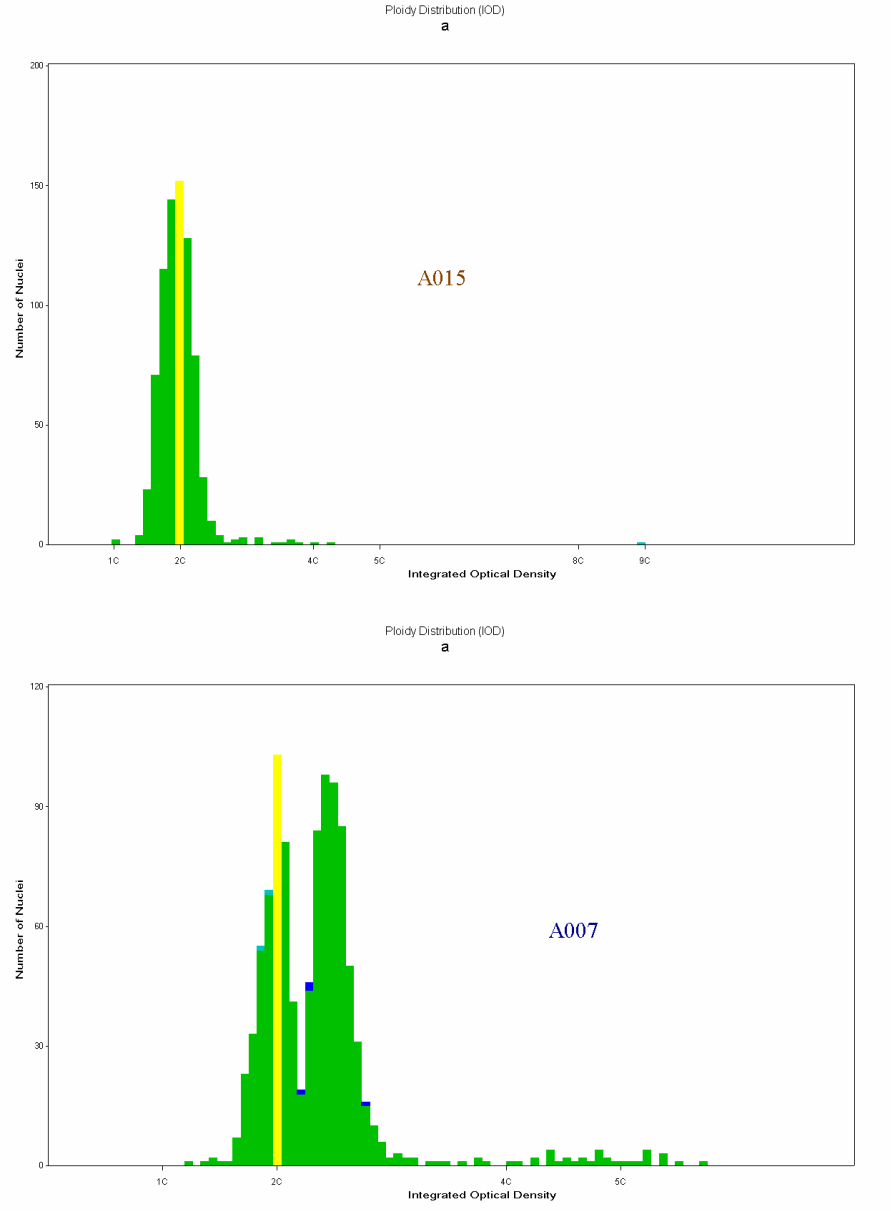

Figure 23. Example DNA histograms from the Fairfield automated image cytometer from study numbers A015 showing a diploid tumour and study number 007, showing an aneuploid tumour.

Results :

Figure 24 shows a plot of the mean normalized and cropped spectra measured from aneuploid and diploid tumours. 35 spectra were measured from 3 aneuploid tumours and 40 spectra measured from 4 diploid tumours. Aneuploid tumours are plotted in blue and diploid tumours in pink. Crude examination of the spectra show apparent differences :
1. In the slope between 400nm and 450nm
2. The mean intensity between 475nm and 550nm
3. The slope between 550nm and 650nm.
There is no perceptible difference in the spectra within the near infra-red region.

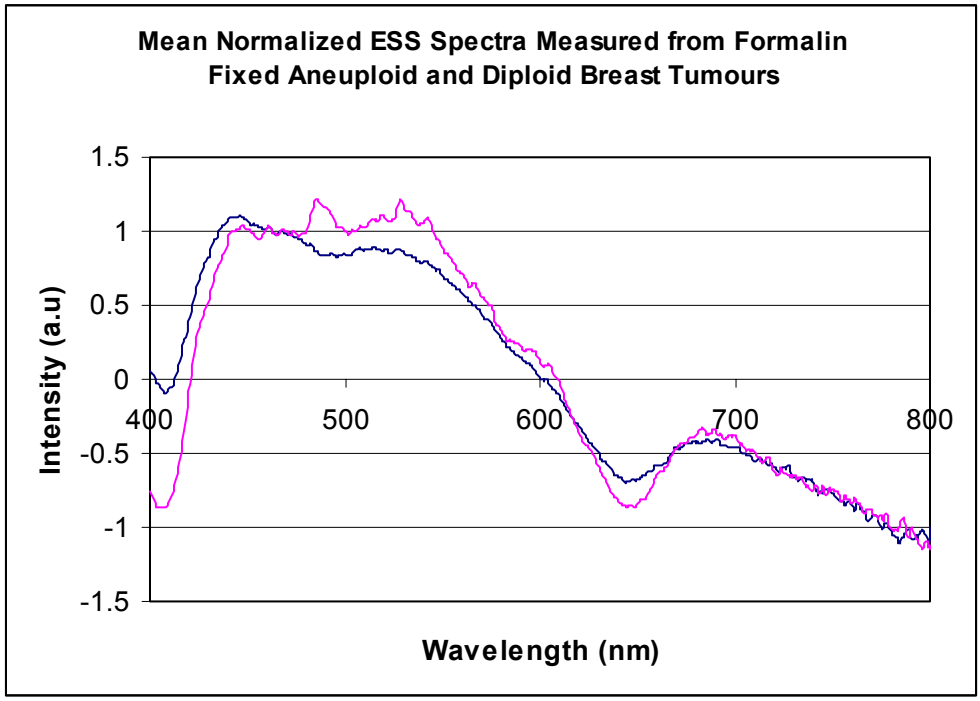

Figure 24 : Mean normalized spectra from Aneuploid breast tumours (pink) and Diploid tumours (Blue).

We need much larger numbers of tumours before attempting to discriminate between diploid and aneuploid tumours using ESS. We plan to continue to recruit to this study, before attempting statistical discrimination.

Of course, our ultimate aim is to detect aneuploidy in vivo using ESS, as this has been shown to have important prognostic implications in breast carcinoma (as well as other cancers).(5-7; 7-9)

CONCLUSIONS FROM ANEUPLOIDY STUDY

1. We have established a laboratory reference procedure for determination of ploidy in breast cancer
2. Measurement of ESS spectra from fresh tissue limited the amount of tissue for analysis, as this was interfering with margin determination by the pathologist.
3. We are continuing to collect ESS spectra from formalin fixed tissue samples to determine ploidy status, though currently do not have enough material analyzed to attempt to perform discriminant analysis.

Objective 4. To develop ductoscopy (nipple endoscopy) to detect intraductal lesions and determine their nature using ESS.

a) To undertake ductoscopy on mastectomy specimens, taking ESS measurements through the endoscope and matching these with biopsies taken by dissection of the tissue
b) To map the distribution of cancer and DCIS around ducts in mastectomy specimens from patients with ductal carcinomas
c) To undertake ductoscopy on patients with nipple discharge, with ESS on any lesions seen to characterize the lesion by spectral analysis

Background :

80% of breast cancers are ductal in origin. Engineering advances have resulted in the production of endoscopes with an external diameter less than 1mm. These micro-endoscopes may be introduced through the nipple to examine the breast ducts, and this procedure is called ductoscopy or nipple endoscopy.

The most promising roles for ductoscopy are:
1. The evaluation of symptomatic nipple discharge – which may be a presenting symptom of breast cancer(10)
2. Early detection of breast cancer – in theory, ductoscopes are capable of visualizing diseased areas as small as 0.2mm, many years before they can be detected with conventional imaging. In addition premalignant lesions (eg. atypical ductal hyperplasia) and ductal carcinoma-in-situ (DCIS) may be visualized(11).
3. Aiding margin determination in breast conserving surgery – by detecting intraductal spread of carcinoma(12).

A key problem is the inability to obtain histological samples for definitive diagnosis of lesions identified at ductoscopy. Our study is to explore the ability of elastic scattering spectroscopy to diagnose pathology seen at ductoscopy. Ductoscopy is carried out by first inserting a thin dilator (like a nylon suture) into a breast duct orifice in the nipple, followed by passing a tubular sheath over this. The dilator can then be removed and the rigid ductoscope passed through the sheath. Unfortunately, the ductoscope is too small to have a biopsy channel and it is not currently possible even to use biopsy forceps through the sheath alone. However, it is practical to pass an ESS probe through the sheath if the ductoscope is removed.

The study was planned in 2 phases :
1. Ex-vivo study: On mastectomy specimens to develop the technique and prove the principle
2. In-vivo study: On patients with symptomatic nipple discharge or diagnosed breast carcinoma. We do not yet have enough data on the ex-vivo study to proceed with the in-vivo study.

Hardware development :

A simple ductoscopy system consisting of ductoscopes and disposable dilators was purchased from RoMC inc, USA.

An ESS optical biopsy probe with external dimensions of 0.8mm, which can be introduced through the ductoscopy sheath, has been produced by our collaborators in Boston, USA. This probe consists of 2 optical fibers with a diameter of 200 microns, with a centre-to-centre separation of 280 microns.

Ductoscopy Procedures :

There is undoubtedly a learning curve for performing ductoscopy. While other authors have reporting accessing up to 5 ducts per breast, to date we have not been able to access any more than 3 ducts for any one patient. The lead surgeon on the program, Mr. Keshtgar, visited Professor William Dooley at the University of Oklahoma and Dr Volker Jacobs in Munich, Germany. Professor Dooley is an internationally acknowledged leader in the development of ductoscopy. Dr Jacobs is investigating autofluorescence for diagnosis of ductoscopically detected pathology. These visits proved extremely valuable for developing technical skills.

To date, we have performed 9 ex vivo ductoscopy procedures on the breast tissue removed from patients undergoing mastectomy for breast carcinoma (7 patients) or prophylactic mastectomy (2 patients) (Fig 25). We have successfully cannulated and examined ducts in 7/9 (78%) of patients. The median number of ducts examined per patient is 2.

The newly developed fiber has been used to measure ESS spectra from normal ducts, hyperplastic ducts, periductal fat, DCIS and invasive cancer. We do not yet have enough spectra to perform an analysis of the ability of the system to detect cancer, but examples of spectra are given in the figure below. Preliminary examination of these spectra shows differences in hemoglobin absorption peaks (compatible with the avascular nature of DCIS) and differences in the spectra within the infra-red region, which may be useful for discrimination (figure 27).

We have developed a method for obtaining conventional tissue biopsies to correlate with the ESS measurements. The ductoscopy light is used either to guide direct tissue biopsies or to mark the duct with a suture, so that a biopsy can be taken when the ductoscopy procedure has been completed (figure 26).

Fig 25. Ex vivo ductoscopy on mastectomy specimen

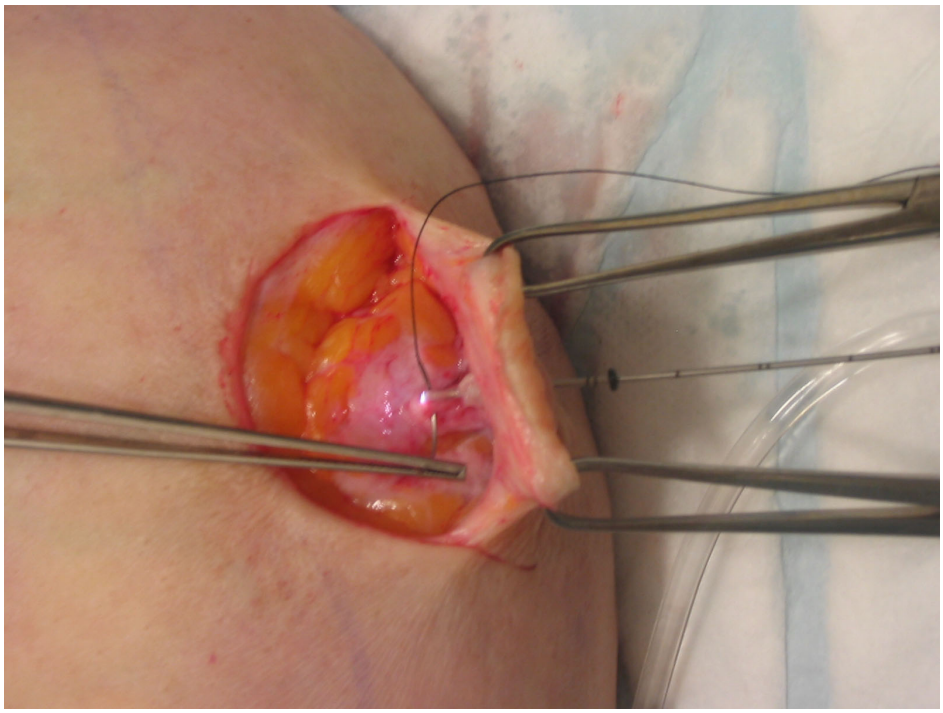

Fig 26. Suture marking of site of ESS measurement

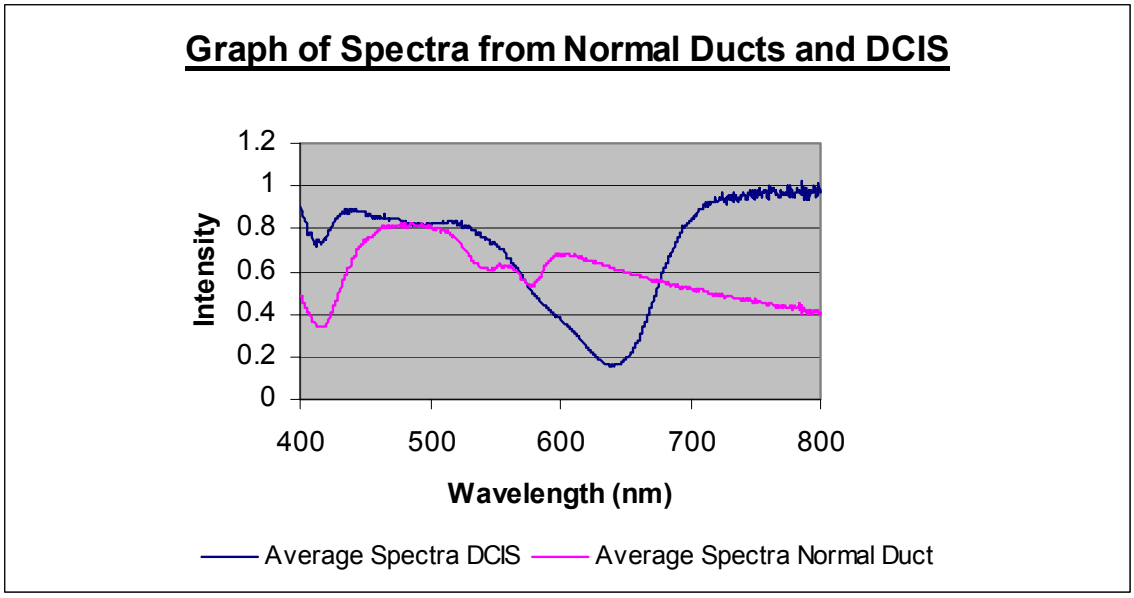

Fig 27. Examples of spectra obtained at ductoscopy from normal ducts (pink) and DCIS (blue)

The next step is to increase the number of ductoscope examinations on ex vivo tissue. If the results are good enough, we shall seek new IRB approval to undertake these measurements in vivo.

Problems encountered :

Initial work was conducted using simple ductoscope, without any working port. Optical biopsies were taken through the dilator used to introduce the ductoscope, after removal of the ductoscope. The duct was then biopsied through percutaneously. It became apparent that, using this methodology, it is very difficult to match the exact site of optical biopsy with the histological samples. The initial ductoscopes used for the study are designed to have a limited lifespan of 5-10 procedures each. Both ductoscopes broke after we had performed 9 procedures.

We had to decide whether to persist with the system used up until this point, or to change to a different ductoscopy system. Ductoscope technology has progressed rapidly during the conduct of the study. Of interest to us was the availability of a more advanced ductoscope from Polydiagnost (Germany) with a working port and with a range of instruments capable of taking pathological samples. This system is of more robust construction than the RoMC system, and designed to be autoclaved. The system is covered by a 2 year warranty and can be repaired if damaged.

The working port within the standard ductoscopes available from PolyDiagnost is, however, too small to introduce our modified ESS probe. We entered into discussion with the engineers from PolyDiagnost who have manufactured a custom built device, with a working port large enough to accept our ESS probe, tiny biopsy forceps or brushes for cytological

examination. We envisage being able to take ESS measurements from pathology under direct vision, followed by a biopsy of the same area. This will enable exact matching of the ESS with the pathology.

The custom built device had just been delivered at the time of preparation of this report and has not yet been used on any patients.

SUMMARY OF DUCTOSCOPY STUDY OUTCOMES

1. The concept of immediate optical diagnosis of pathology seen at ductoscopy is attractive and has been welcomed by those working within the field.
2. We have developed the technical skills to perform ductoscopy.
3. We have built a probe capable of taking ESS measurements.
4. We have started collecting spectra with matched histology. At this stage, cursory examination of the spectra has shown clear differences between normal ducts and cancer. The number of measurements is currently too low to attempt statistical discrimination.
5. We have had a device custom built to continue this study to achieve the necessary data to reach conclusions on the ability of ESS to discriminate between pathology encountered at ductoscopy.
6. We plan to proceed to an in-vivo study once satisfied that we are able to discriminate between pathology in the ex-vivo study.

KEY RESEARCH ACCOMPLISHMENTS

1. We have demonstrated the ability of ESS to differentiate between cancer and normal breast tissue with high specificity and sensitivity.

2. We have demonstrated that ESS retains this ability to detect cancer, even when only a small percentage of the tissue volume interrogated by the light pulse is cancer.

3. We have expanded our database of ESS spectra from sentinel and other axillary nodes with matched histology and have further revised the algorithm for analysis of these spectra.

4. We have addressed the problem of sampling errors leading to cancer in sentinel nodes failing to be detected by using a prototype 2-dimensional scanning device that can scan an area of 1cm^2 on the cut surface of nodes within 12 minutes.

5. Using the scanner, we have shown that the sensitivity and specificity for detecting cancer in sentinel nodes is almost exactly the same as touch imprint cytology, but without the need for tissue processing or a pathologist to interpret the scans.

6. We have optimized the methodology for DNA ploidy determination using image cytometry and are starting to build a database to correlate ESS spectra with image cytometry, looking for algorithms to detect aneuploidy from the spectra.

7. We have developed an optical probe that is able to measure ESS spectra at ductoscopy and developed methodology for matching histology with these spectra. We are recruiting patients to this study.

REPORTABLE OUTCOMES

Peer-reviewed Published Papers in Scientific Journals

Elastic scattering spectroscopy for intraoperative determination of sentinel lymph node status in the breast. Johnson KS, Chicken DW, Pickard DCO, Lee AC, Briggs G, Falzon M, Bigio IJ, Keshtgar MR, Bown SG. Journal of Biomedical Optics 9 (6): 1122-1128 Nov-Dec 2004

A Training Simulator for Sentinel Node Biopsy in Breast Cancer: a New Standard. Keshtgar, M. R. S., Chicken, D. W., Waddington, W. A., Raven, W., & Ell, P. J. European Journal of Surgical Oncology 2005;31:134-140

Monitoring Recovery After Laser Surgery of the Breast With Optical Tomography: a Case Study. Hebden, J. C., Yates, T. D., Gibson, A., Everdell, N., Arridge, S. R., Chicken, D. W., Douek, M., & Keshtgar, M. R. S. Applied Optics 2005;44:1898-1904

Elastic Scattering Spectroscopy for Detection of Sentinel Lymph Node Metastases in Breast Carcinoma. DW Chicken, AC Lee, KS Johnson, B Clarke, M Falzon, IJ Bigio, SG Bown, MRS Keshtgar. SPIE Proceedings, 2005;5862:66-73

New Approaches in Breast Cancer Management: Sentinel Node Biopsy and Intraoperative Radiotherapy. Keshtgar, M. R., Chicken, D. W., & Tobias, J. S. International Journal of Fertility and Womens Medicine. 2005;50:218-226

Intraoperative Touch Imprint Cytology for the Diagnosis of Sentinel Lymph Node Metastases in Breast Cancer. Chicken, D. W., Kocjan, G., Falzon, M., Lee, A. C., Douek, M., Sainsbury, R., & Keshtgar, M. R. British Journal of Surgery. 2006;93:572-576

Patients' View on Intraoperative Diagnosis of Sentinel Nodes in Breast Cancer: Is It an Automatic Choice? Chicken, D. W., Sivanandrajah, N., Keshtgar, M. R. S. International Journal of Surgery 2006;4 (Published online ahead of print)

Other peer reviewed publications on Elastic Scattering Spectroscopy from work undertaken by members of the breast team in collaboration with other projects in the National Medical Laser Centre

Elastic scattering Spectroscopy for detection of dysplasia in Barrett's Oesophagus. Lovat L, Bown S. Gastrointest Endosc Clin N Am. 2004 Jul;14(3):507-17.

Elastic scattering spectroscopy for the diagnosis of colonic lesions: initial results of a novel optical biopsy technique. Dhar A, Johnson KS, Bown SG, Bigio IJ, Lovat LB, Bloom SL. Gastrointest Endosc. 2006 Feb;63(2):257-61.

Elastic scattering spectroscopy accurately detects high grade dysplasia and cancer in Barrett's esophagus. Lovat LB, Johnson K, Mackenzie GD, Clark BR, Novelli M, Davies S, O'Donovan M, Selvasekar C, Thorpe SA, Pickard D, Fitzgerald R, Fearn T, Bigio IJ, Bown SG. GUT (published on line 2006)

Presentations with Abstracts Published in Scientific Journals

27th Annual San Antonio Breast Cancer Conference, San Antonio, Texas. USA, 8th-11th December 2004: Poster : Optical biopsy utilizing elastic scattering spectroscopy for the intraoperative determination of sentinel node status in breast carcinoma. Chicken DW, Johnson KS, Bown SG, Bigio IJ, Keshtgar MRS
Abstract : Breast Cancer Research and Treatment 88: S87-S88 Suppl. 1 2004

27th San Antonio Breast Cancer Symposium, San Antonio, Texas, USA: Clinical Skills Laboratory Training in Sentinel Node Biopsy in Breast Cancer - The Development of a Simulator Keshtgar, M. R. S., Chicken, D. W., Waddington, W., & Ell, P. J.
Abstract : Breast Cancer Research and Treatment 2004;88:S81-S82

Association of Surgeons of Great Britain & Ireland Annual Scientific Meeting, Glasgow, UK. April 2005, Poster & presentation : Trainees' Evaluation of a Simulator for Sentinel Node Biopsy in Breast Cancer: a New Standard. Keshtgar, M. R. S., Chicken, D. W., Waddington, W., & Ell, P. J
Abstract : British Journal of Surgery 2005;92:71-71

9th Nottingham International Breast Cancer Conference, Nottingham, UK.. Intra-operative Touch Imprint Cytology of Clinically Apparent Sentinel Node Metastases : Why Bother?. Oral presentation. Chicken, D.W., Falzon, M., Kocjan,G., Douek,M., Sainsbury,J.R.S., Keshtgar,M.R.S.
Abstract : European Journal of Cancer 2005;3(1), 31-31

28th San Antonio Breast Cancer Symposium, San Antonio, Texas, USA: Optical Biopsy: Breast Cancer Diagnoses at the Speed of Light. Poster. Chicken DW, Clark BR, Johnson KS, Lee AC, Briggs G, Pickard CDO, Falzon M, Novelli M, Bown SG, Bigio IJ, Keshtgar MRS
Abstract : Breast Cancer Research and Treatment 2005;94:S43-S43

Forthcoming Presentation : *4th International Congress on MR Mammography, Jena, Germany, Sept 2006* : Rapid Intraoperative Diagnosis of Sentinel Node Metastases in Breast Cancer using Elastic Scattering Spectroscopy Scanning D.W. Chicken, B. Clark, A. Mosse, M. Falzon, G. Kocjan, M.R.S. Keshtgar, S.G. Bown
Abstract: To be published in "European Radiology" (September 2006).

Forthcoming Presentation : *British Association of Surgical Oncology - Association for Cancer Surgery Scientific Meeting, London, UK, November 2006.* Platform presentation : Rapid Intraoperative Diagnosis of Sentinel Node Metastases in Breast Cancer using Elastic Scattering Spectroscopy Scanning. D. Chicken, B Clark, A Mosse, M Falzon, G Kocjan, S Bown, M Keshtgar.
Abstract : To be published in European Journal of Surgical Oncology, November 2006.

Additional Published Scientific Abstract

ASCO (American Society of Clinical Oncology) meeting 2004
Optical biopsy utilising elastic scattering spectroscopy for intra-operative diagnosis of sentinel lymph node metastases. Chicken DW, Johnson KS, Falzon MR, Lee AC, Briggs G, Pickard D, Bigio IJ, Bown SG, Keshtgar MRS. Journal of Clinical Oncology 22 (14): 841 Suppl. S JUL 15 2004

Presentations with Abstracts published only in Conference Programs or with no Published Abstract

European Conference on Biomedical Optics, Munich, Germany, 12th – 16th June 2005, Munich, Germany. Elastic Scattering Spectroscopy for Detection of Sentinel Lymph Node Metastases in Breast Carcinoma. DW Chicken, AC Lee, KS Johnson, B Clark, M Falzon, IJ Bigio, SG Bown, MRS Keshtgar.

4th International Sentinel Node Conference, Santa Monica, California, USA, 3rd-6th December 2004 : Poster : Instantaneous detection of sentinel node metastases in breast cancer by "optical biopsy" using elastic scattering spectroscopy**.** D. Chicken, K Johnson, M Falzon, W. Waddington, P. Ell, S Bown, M Keshtgar.

4th International Sentinel Node Conference, Santa Monica, California, USA, 3rd-6th December 2004 : Platform presentation : Comparing the Performance of Intraoperative Probes with a Gamma Camera - Which is better at detecting weakly active, deeper Sentinel Nodes? W. Waddington, DW Chicken, MRS Keshtgar

British Medical Laser Association Autumn Meeting, 9th & 10th September 2004,
London, UK. Platform presentation: The application of light in the diagnosis and management of breast disease. MRS Keshtgar, DW Chicken

4th International Symposium on the Intraductal Approach to Breast Cancer, 11th-13th March 2005, Santa Barbara, California, USA. Platform presentation : Light for Lightning Diagnosis. MRS Keshtgar

US Army Era of Hope Conference, June 8th-11th 2005, Philadelphia, Pennsylvania, USA. Platform presentation and poster: Poster and platform presentation : Optical Biopsy for Real-time Diagnosis, Staging and Prognostication in Breast Cancer. M Keshtgar, D Chicken, A Lee, G Briggs, K Johnson, B Clark, D Pickard, M Falzon, I Bigio & S Bown

Society of Academic & Research Surgeons Annual Conference, Edinburgh, UK. January 2006. Poster presentation: Elastic scattering Spectroscopy : A Rapid Optical Technique for the Detection of Sentinel Node Metastases. DW Chicken, B Clark, KS Johnson, M Falzon, IJ Bigio, SG Bown, MRS Keshtgar.

Other Publications

Conference Report : The 4th Biennial International Sentinel Node Congress, 3-6th December, Los Angeles, California. Chicken, D. W. & Keshtgar, M. R. S. Eur J Nucl Med Mol Imaging 2005;32:375-376

Letter : Allergic Reactions to Patent Blue Dye. Mansouri, R , Chicken, DW & Keshtgar, MRS. Surgical Oncology. Accepted for publication.

Submission of Higher Degrees

1. Wayne Chicken will be submitting a doctoral thesis in 2006 to the University of London based on the work performed under this grant.

2. Ying Zhu, a PhD student in statistics, will be submitting a PhD thesis to the University of London based in part on work performed during this program

CONCLUSIONS

Elastic scattering spectroscopy is a relatively simple and low cost technique, which has the potential to provide an immediate answer as to whether or not cancer is present in breast or lymph node tissue. As the spectra are analyzed by computer algorithm, no pathological interpretation is required, so the results are essentially operator independent. Our results so far have shown good sensitivity and specificity for detecting cancer, but there is considerable potential for developing the technique further.

The key limitations of the technique at present are:

1. The speed of scanning. The early prototype took 40 minutes to scan $1cm^2$. This needs to be greatly reduced for the technique to be clinically useful as it will be necessary to scan several surfaces for exhaustive interrogation of all nodes. We have succeeded in reducing the scanning time to 12 minutes at the time of this report.
2. The result is presented as a scan. Further automation may make it possible to give the result just as "cancer present" or "cancer absent" in a node.
3. Increasing the data base of data pairs (correlated spectra and conventional histology) may improve the accuracy of the diagnostic algorithm
4. It is not known exactly how deep into the tissue ESS can detect cancer. This is likely to be in the range of 0.3-0.5mm. This will determine how thick slices of tissue need to be for ESS to be able to interrogate every part of a sentinel node.

This program has taken the first steps towards assessing ESS for 2 new applications – detecting aneuploidy and diagnosing lesions seen at ductoscopy. It is hoped that these potential uses of this technique can be explored further in future research programs.

"SO WHAT?"

We have developed ESS scanning of axillary lymph nodes to the point where we have demonstrated that its sensitivity and specificity for detecting cancer is comparable to conventional techniques (touch imprint cytology and frozen section histology), but with the potential for an almost immediate result and without the need for a pathologist to interpret the findings. The technique is now ready for prospective testing and if this is successful, could be adopted very cost effectively in any centre undertaking surgery for breast cancer, using equipment that is rugged and relatively cheap. ESS scanning also has considerable potential for the immediate detection of cancer, *in vivo* or *ex vivo*, in a wide range of tissues other than the breast.

REFERENCE LIST

(1) Bigio IJ, Mourant JR. Ultraviolet and visible spectroscopies for tissue diagnostics: fluorescence spectroscopy and elastic-scattering spectroscopy. Phys Med Biol 1997; 42(5):803-814.

(2) Mourant JR, Canpolat M, Brocker C, Esponda-Ramos O, Johnson TM, Matanock A et al. Light scattering from cells: the contribution of the nucleus and the effects of proliferative status. J Biomed Opt 2000; 5(2):131-137.

(3) Mourant JR, Hielscher AH, Eick AA, Johnson TM, Freyer JP. Evidence of intrinsic differences in the light scattering properties of tumorigenic and nontumorigenic cells. Cancer 1998; 84(6):366-374.

(4) Chicken DW, Kocjan G, Falzon M, Lee AC, Douek M, Sainsbury R et al. Intraoperative touch imprint cytology for the diagnosis of sentinel lymph node metastases in breast cancer 1. Br J Surg 2006; 93(5):572-576.

(5) Moureau-Zabotto L, Bouchet C, Cesari D, Uzan S, Lefranc JP, Antoine M et al. Combined flow cytometry determination of S-phase fraction and DNA ploidy is an independent prognostic factor in node-negative invasive breast carcinoma: analysis of a series of 271 patients with stage I and II breast cancer. Breast Cancer Res Treat 2005; 91(1):61-71.

(6) Silvestrini R, Daidone MG, Del Bino G, Mastore M, Luisi A, Di Fronzo G et al. Prognostic significance of proliferative activity and ploidy in node-negative breast cancers. Ann Oncol 1993; 4(3):213-219.

(7) Haffty BG, Toth M, Flynn S, Fischer D, Carter D. Prognostic value of DNA flow cytometry in the locally recurrent, conservatively treated breast cancer patient. J Clin Oncol 1992; 10(12):1839-1847.

(8) Moureau-Zabotto L, Bouchet C, Cesari D, Uzan S, Lefranc JP, Antoine M et al. Combined flow cytometry determination of S-phase fraction and DNA ploidy is an independent prognostic factor in node-negative invasive breast carcinoma: analysis of a series of 271 patients with stage I and II breast cancer. Breast Cancer Res Treat 2005; 91(1):61-71.

(9) Silvestrini R, Daidone MG, Del Bino G, Mastore M, Luisi A, Di Fronzo G et al. Prognostic significance of proliferative activity and ploidy in node-negative breast cancers. Ann Oncol 1993; 4(3):213-219.

(10) Dooley WC. Routine operative breast endoscopy for bloody nipple discharge. Ann Surg Oncol 2002; 9(9):920-923.

(11) Dooley WC. Ductal lavage, nipple aspiration, and ductoscopy for breast cancer diagnosis. Curr Oncol Rep 2003; 5(1):63-65.

(12) Dooley WC. Routine operative breast endoscopy during lumpectomy. Ann Surg Oncol 2003; 10(1):38-42.

APPENDIX : LIST OF PERSONNEL WHO CONTRIBUTED TO US ARMY PROJECT GSG7

Stephen BOWN	PI
Wayne CHICKEN	Clinical Research Fellow
Kristie JOHNSON	Physicist
Benjamin CLARK	Physicist
Martin AUSTWICK	Physicist
Mary FALZON	Pathologist
Mohammed KESHTGAR	Breast Surgeon
Ying Zhu	PhD student in statistics